Lauri Syväranta

A Tool for Solar Plant Optimization

Department of Electrical Engineering

Thesis submitted for examination for the degree of Master of Science in Technology.

Espoo 24.2.2011

Thesis supervisor:

Prof. Seppo Ovaska

Thesis instructor:

D.Sc. Konstantin Kostov

Aalto University
School of Electrical
Engineering

AALTO-YLIOPISTO
SÄHKÖTEKNIIKAN KORKEAKOULU

DIPLOMITYÖN
TIIVISTELMÄ

Tekijä: Lauri Syväranta

Työn nimi: Aurinkovoimalan optimointityökalu

Päivämäärä: 24.2.2011 Kieli: Englanti Sivumäärä:6+47

Sähkötekniikan laitos

Professuuri: Tehoelektroniikka Koodi: S-81

Valvoja: Prof. Seppo Ovaska

Ohjaaja: TkT Konstantin Kostov

Tässä diplomityössä tutkitaan suuritehoisia verkkoonkytkettyjä aurinkovoimaloita ja niiden tehoelektronisten järjestelmien kykyä muuntaa energiaa vuoden mittaan esiintyvissä auringonpaiste- ja lämpötilaoloissa. Työssä tarkastellaan keskitettyjä jännitevälipiirivaihtosuuntaajia, joiden välipiiriä syötetään yhdellä keskitetyllä tai useammalla hajautetulla nostavalla katkojalla. Myös katkojatonta, muuntajallista vaihtoehtoa tutkitaan.

Aluksi käydään läpi aurinkopaneelien perusominaisuudet ja osoitetaan, että olosuhteiden vaihtelut vaikuttavat merkittävästi paneelien toimintaan. Myös paneelien sarjaan- ja rinnankytkennästä aiheutuvat ilmiöt selvitetään, sillä tyypillisesti yksittäisen paneelin lähtöteho on pieni verrattuna optimaalisen vaihtosuuntaajan kokoon.

Työssä tarkastellaan erityisesti osittain varjostuneita ja vioittuneita paneelistoja, joiden energiansaannin optimointi on erityisen haastavaa. Tähän tarkoitukseen esitellään työkalu, jolla voidaan selvittää voidaanko hajautetuilla katkojilla saavuttaa merkittävää etua energiansaannissa keskitettyyn katkojaan verrattuna. Oletuksena on, että aurinkopaneeliston huipputehon seuranta on toteutettu katkojassa, jolloin hajautettujen katkojien käyttö johtaa tarkempaan seurantaan, jos paneeliston osat ovat eri toimintapisteissä.

Aurinkovoimayrittäjän näkökulmasta ongelma on, tuottaako kallis ja monimutkainen järjestelmä suurempien kustannustensa vastineeksi yksinkertaista järjestelmää paremman tuoton. Tähän ongelmaan esitetään ratkaisutapa.

Avainsanat: aurinkoenergia, aurinkopaneeli, verkkovaihtosuuntaaja, aurinkovoimala

AALTO UNIVERSITY
SCHOOL OF ELECTRICAL ENGINEERING

ABSTRACT OF THE
MASTER'S THESIS

Author: Lauri Syväranta

Title: A Tool for Solar Plant Optimization

Date: 24.2.2011 Language: English Number of pages:6+47

Department of Electrical Engineering

Professorship: Power Electronics Code: S-81

Supervisor: Prof. Seppo Ovaska

Instructor: D.Sc. Konstantin Kostov

The topic of this thesis is large scale photovoltaic energy production and the power electronic converters involved. The power electronic systems' ability to harvest the energy provided by a solar panel installation formed the main investigation. The converter configurations considered are the single stage inverter, the inverter fed by a centralized boost converter or decentralized boost converters, and the inverter with a grid frequency transformer.

The basic properties of photovoltaic panels and their series and parallel connections are discussed briefly. It is shown that environmental changes have considerable effect on the panels' and thus the whole system's ability to produce energy, especially when panels are connected in series and in parallel, which is often the case in large scale production.

Partially shaded or malfunctioning installations are under special consideration because of the challenges they introduce to optimizing the energy output. This thesis describes a tool for comparing the energy yield of different converter configurations under varying conditions, such as temperature, insolation, and partial shading.

The interest of someone planning to invest in photovoltaic energy production would naturally be whether the added cost of more complex configurations is justified. Is the energy yield considerably better? This thesis provides a tool for answering these questions.

Keywords: Solar plant, solar energy, photovoltaic panel, solar inverter

Preface

This thesis was made as a part of a project in the Aalto University School of Electrical engineering funded by Tekes and Vacon Plc (Vaasa, Finland). I want to thank Hannu Sarén at Vacon for his support and bringing this extremely interesting field of engineering to my attention.

I want to thank my instructor D.Sc. Konstantin Kostov and my supervisor Prof. Seppo Ovaska for their patience and guidance in the process of making this thesis. Due to special personal circumstances, extra patience and flexibility was needed. At a crucial point in preparing this thesis, there was a fire in our apartment. Luckily, the renovations took less time to finalize than this thesis, so we have been able to enjoy our new home for some time now.

My parents Hilve and Seppo deserve a lot of credit for supporting me morally and sometimes financially in my studies. I also have fond memories of my uncle Olli Varhomaa, the first M.Sc. in the family. It is his example that led me to this fine university in the first place. I greatly regret not being able to celebrate my future graduation with him, since he passed away suddenly some four years ago.

Last, but most, I want to thank my beloved wife Suvi for her love, patience, and understanding. This thesis has been in the making for long enough, but waking up with her every day has made the time pass as if on wings.

Otaniemi, 24.2.2011

Lauri Syväranta

Contents

Abbreviations and symbols

Abbreviations

AC	alternating current
DC	direct current
MPP	maximum power point, i.e. the operating point at which a photovoltaic panel produces the maximum power
MPPT	maximum power point tracker or tracking
pV	photo Voltaic
PWM	pulse width modulation
RMS	root mean square
VBA	Microsoft Visual Basic for Applications

Symbols

η	efficiency
i	current
u	voltage
I	DC or RMS-current
U	DC or RMS-voltage
k	the Boltzmann constant
T	absolute temperature
S	insolation
q	the elementary charge

Operators

$\hat{\eta}$	an approximation of the variable η
$\frac{dU}{dT}$	the derivative of U with respect to T

1 Introduction

Solar power as a form of renewable energy is an extremely popular topic in contemporary electrical engineering. The break-even point of the energy production has been reached, a photovoltaic (pV) panel built today will produce more energy than needed to manufacture it. Richards even states that this has been the case for all but the first pV panels built for space applications several decades ago [1]. Nevertheless, the solar boom has started as many western countries subsidise solar energy heavily, even guaranteeing a fixed feed-in tariff for decades to come. As a result, solar energy production has become a lucrative and in some cases risk-free business.

In order to feed the DC-current produced by the pV-panels to the AC-grid, power electronic converters have to be used. This opens a market for inverter manufacturers: all pV-power plants must use an inverter at one stage or another. The manufacturers have no easy task trying to accommodate the needs of the system integrators, who build power plants from the individual components. There is little or no standardization to aid them. The legislation and standards concerning pV-power production that do exist vary between market areas.

Power conversion may appear trivial, since it is easy enough to produce a steady alternating current (AC) from a constant direct current (DC) voltage source. The pV-module, however, does not produce a constant DC-voltage or current, at least not in the time frame of hours, let alone days. The voltage and current produced by a pV-module depend mainly on two environmental parameters: insolation and temperature. Neither would be of consequence were it not for the limits introduced by legislation and panel ratings; most panel manufacturers have their panels rated for 1000V in Europe and 600V in the United States of America (USA) [2].

It is generally accepted that the voltage at the maximum power point (MPP) of a panel is approximately 80 % of the open circuit voltage (V_{OC}) [3]. This means that to maximize the energy production the DC-link voltage of the inverter can be no more than 800V. V_{OC} is approximately inversely proportional to the junction temperature of the panel resulting in the voltage being at its minimum on hot days [4, p. 137]. It is unfortunate that hot days are when insolation tends to be at its greatest and the most energy would be available.

If the V_{OC} may not exceed 1000V at standard test conditions (STC), where the panel temperature is 25°C, the case may easily be that on a hot day, with the sun shining on the dark panels causing their temperature to rise well above the ambient temperature, the MPP-voltage falls under 625V. At this point a sinusoidal 400V line-to-line AC-voltage can no longer be produced at the MPP of the pV-module without an additional boost converter or step-up transformer.

The inversely proportional nature of the voltage and temperature of a photovoltaic module is an inconvenient feature also in another sense: regions that enjoy the most insolation also tend to be the hottest areas. Since high temperatures cause the voltage and thus the power to drop, this would suggest that the hottest, sunniest places might not be the optimal locations for a photovoltaic power plant. Indeed, other methods for harvesting power more or less directly from solar radiation also

exist, and have been in use for decades. These methods are based on concentrating solar radiation to produce heat. The heat is used in traditional heat engines or Stirling engines to produce electrical power with rotating generators. The downside of these methods is the need of large amounts of fresh water, a scarce resource in many sunny regions [5], although Stirling engines are better in this regard.

Many papers discuss the efficiency of different converter configurations for photovoltaic energy harvesting. Fewer papers, however, take into account the effect the converter has on the total energy yield of the installation in the course of a year, let alone the lifetime of the installation. The ratio of the actual energy yield and the installation cost, the return on investment, is ultimately the most important parameter investors will be concerned about.

Literature suggests the use of astronomical calculations to determine the insolation at a specific location [3, p. 6 - 18]. During the course of our study we found that temperature data is almost as important as insolation data, perhaps even more so. This is why we aimed to use actual measurement data of both insolation and temperature. A previous study using actual measured insolation and temperature data has been made by G. Walker in the University of Queensland, Australia in 2001 [6]. Walker concentrates on low voltage standalone installations, where only one pV panel is considered, while this thesis concentrates on large grid connected installations. While Walker uses actual insolation and temperature data and considers the energy yield over a long time period, his study is not useful for determining the benefits of larger installations. Another improvement in this thesis is that accurate efficiency data of the compared configurations are used.

A study on the partial shading of pV-arrays has been made by H. Patel and V. Agarwal [7]. Where Walker only considers one solar panel over a long period of time up to a whole year, Patel and Agarwal consider an entire array of solar panels, but time frames of only one second. Both Walker and Patel & Agarwal use Matlab (Mathwors Inc., Natick, MA, USA) to simulate their cases. The nature of this thesis is more practical: more readily available software is used to simulate a combination of the previously mentioned studies and simulate an array of solar panels over a long period of time. Also, the behaviour of the pV-panel array is only one point of interest, a more important one being the ability of different power electronic converters to harvest as much of the energy produced by the panels as possible.

The aim of this thesis is not to find the optimal configuration for all locations; this would be impossible since environmental conditions have dramatic geographical variance. Therefore, an optimal solution in some area or installation size might be less than satisfactory in another. A tool is presented in Section 3 that can be used for such comparisons by anyone who needs unbiased information about the actual energy yield of different configurations and knows what kind of environment they are operating in.

The efficiencies of three inverters were measured in addition to reviewing published efficiency measurements to test the tool with realistic data. To make the comparison as easily repeatable as possible, readily available office tools were used instead of expensive scientific software. All data used in the comparison, save the

efficiency measurement data of the inverters, is readily available to anyone. As far as the inverters go, the measurements will also show that the efficiencies claimed by the manufacturers are reasonably accurate and could also be used in such a comparison.

A point of interest to anyone planning to invest in a solar plant is surely to find whether the higher energy yield of more complex configurations warrants the added installation cost. The optimal power level of a production unit would also be of great interest. This thesis does not aim to answer these questions directly but it gives tools to find the optimal solution in a given environment. It is also shown that environmental variables such as climate and legislation have such a large effect on the system that a universal optimum is very unlikely to exist.

The solar inverter configurations considered in this thesis are the central inverter configuration with or without a grid transformer, the central inverter configuration with additional DC-boost converters, and the module inverter. In the central inverter configuration enough pV-panels are connected in series to raise the voltage to such a level that a 3-phase AC-voltage can be achieved, sometimes an additional 3-phase grid transformer is used to raise the voltage. The central inverter with a DC-boost converter consists of one or several strings of panels connected to a DC-boost converter, and one or several of such DC-boost converters connected to a centralized inverter. The final configuration, the so called module inverter, consists of small inverters that include a DC-boost stage. The module inverters are intended to handle the power produced by a single pV-panel and will only be discussed in the theoretical part of this thesis.

2 Background

The basic concepts of photovoltaic energy production will be discussed in this section. The first topic is the behaviour of solar panels, consisting of multiple pV-cells. The terms solar panel and pV-module are equal in meaning, and will be used interchangeably throughout this thesis.

The power electronic converters associated with solar power will be discussed in the subsequent part and, finally, an inverter efficiency measurement set-up and results to validate manufacturer claimed efficiency data are presented in the last part of this section.

2.1 Behaviour of photovoltaic cells

When a photovoltaic panel is illuminated, the photons from the light source are absorbed by electrons in the panel. Some of these electrons absorb enough energy to be excited from the valence band of the semiconductor to the conduction band. This process causes a build up of opposite charges at opposite ends of the panel. When connected to a circuit, the panel will thus act as a current source. The equivalent circuit model of a pV-cell is represented in Figure 1. [4, p. 132]

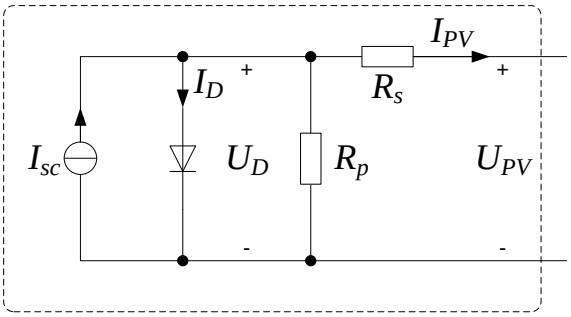

Figure 1: Equivalent circuit of a pV-cell

It can be deduced from Figure 1 that the current produced by the module is

$$I_{PV} = I_{SC} - I_D - \frac{U_D}{R_p} \ . \tag{1}$$

The current I_{SC} is directly proportional to the solar radiation, or insolation, that falls on the cell. The diode can be modelled with the Shokley diode equation [8] presented in (2):

$$I_D = I_S \left(e^{qU_D/\phi kT} - 1 \right) \ , \tag{2}$$

where

$$\begin{aligned} I_S &= \text{reverse saturation current} \\ k &= \text{the Boltzmann constant} \\ q &= \text{The elementary charge} \\ U_D &= \text{Diode voltage} \\ \phi &= \text{Diode ideality factor} \\ T &= \text{Absolute temperature.} \end{aligned}$$

Assuming that the parallel resistance R_p is so large that negligible current flows through it and substituting (2) into (1) we can derive the following equation for the cell current. The voltage drop across R_s is also assumed negligible.

$$I_{PV} = I_{SC} - I_S \left(e^{qV_D/\phi kT} - 1 \right) \ . \tag{3}$$

We can now plot the current as a function of voltage. This curve is called the characteristic curve of the pV-cell. If cells are connected in series and parallel, as they would be in a pV-module, i.e. a solar panel, the voltages and currents can be summed assuming that the whole panel is in the same insolation and temperature conditions. The characteristic curves of a typically sized module at three different insolation levels are plotted in Figure 2.

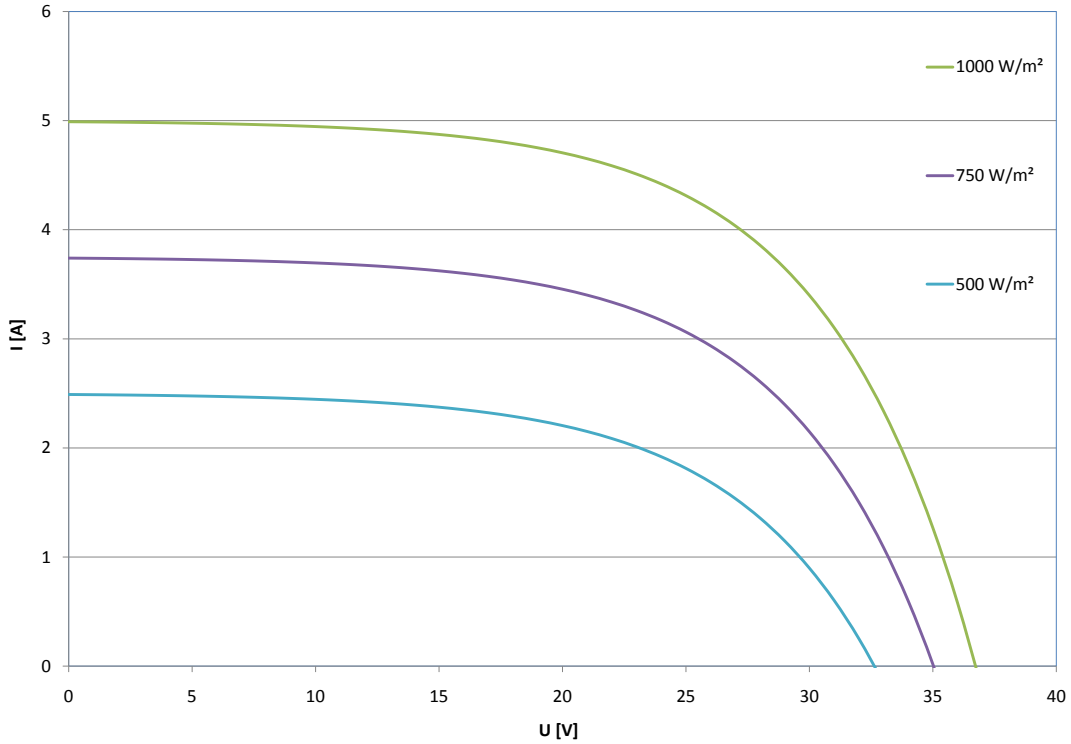

Figure 2: pV-module current as a function of voltage

The temperature of the panel, or more precisely the diode junction temperature, also affects the voltage-current curve of the panel. The common practical approach

to take this effect into account is by using temperature coefficients. The typical values for silicon and germanium diodes are

$$\frac{dV}{dT} = -2.3 \ldots - 2.1 mV/^{\circ}C \ . \tag{4}$$

It is worthwhile to note that the coefficient is negative. This means the higher the temperature, the lower the voltage [4, p. 135]. The dependency can be considered linear. An even more practical approach is to provide the coefficient as a percentage. This way the constant stays the same regardless of the amount of panels connected in series. The voltage as a function of temperature can thus be found according to (5).

$$V\left(T\right) = V_0 \left[1 + \left(T - T_0\right) K_V\right] \ , \tag{5}$$

where

$$K_V = \frac{dV}{dT} \cdot 100\% \tag{6}$$

The value K_V can be found on most pV-panel data-sheets; BP Solar (BP Solar International Inc, San Francisco, CA, USA) provides a value of 0.36%/°C for their BP 3230T solar panel [2]. The effect temperature has on voltage and thus the UI-curve of the panel is depicted in Figure 3.

A study has also been made by T. Nordmann and L. Clavadetscher on the effect of solar radiation on the panel temperature in different kinds of installations [9]. According to the study, the temperature of the panel may rise between 20°C and 55°C above ambient per kW/m^2 of insolation. This means that the panel temperature will be between 45°C and 80°C on a 25°C day at 1000 W/m^2 solar irradiation.

Environmental factors clearly have a large effect on solar panel behaviour. This is why panel specifications are given in standardized conditions. Two sets of environmental parameters have been standardized in IEC 60904-3. Standard test conditions (STC) are defined so that panel temperature is 25°C, insolation is 1000 W/m^2, and ambient temperature is not defined. Normal operating conditions (NOC) are defined so that ambient temperature is 20°C, wind speed is 1m/s, and insolation is 800 W/m^2 [10].

The power produced by the module, the product of voltage and current, also changes as a function of voltage. The power produced by the previous module is represented in Figure 4 as a function of voltage.

A clear maximum can be seen in the power output. This maximum is the MPP of the panel. The voltage and current of the panel at this point are usually given in the data-sheets of solar panels. This point, however, does not stay constant: the voltage and current change as a function of both insolation and temperature. As described above, insolation mostly affects current and temperature mostly affects voltage.

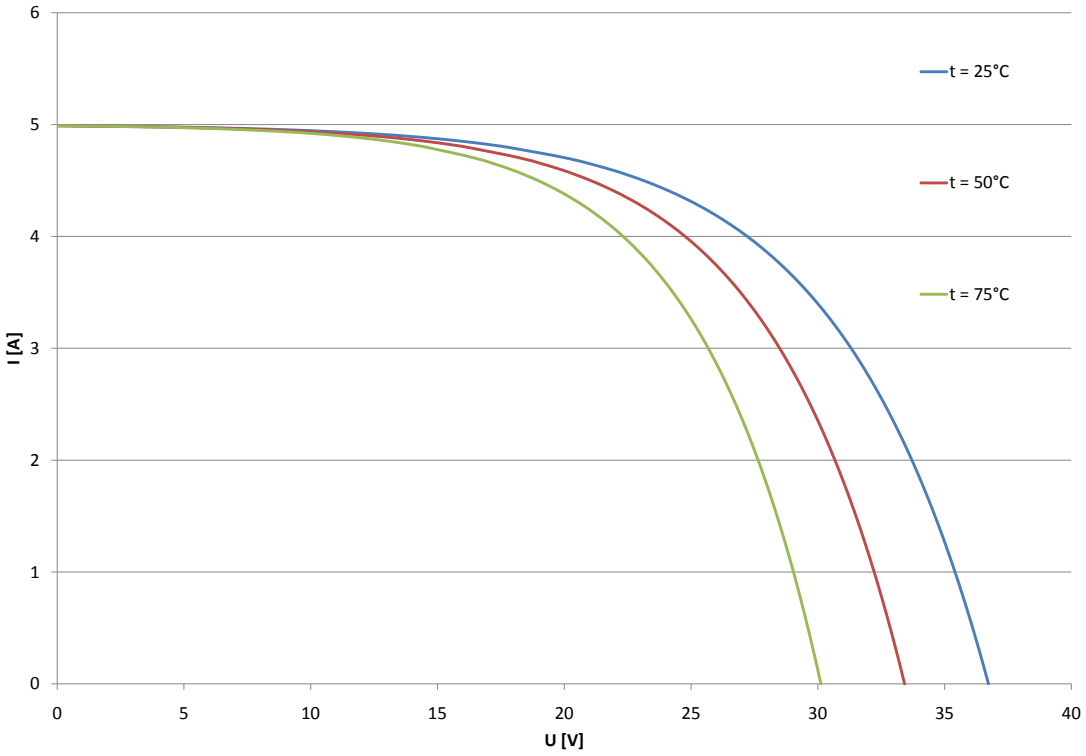

Figure 3: pV-module current as a function of voltage at different panel temperatures

Since the MPP does not remain constant in the likely operating conditions of a solar panel, the power converter used to extract power from the pV-module should have some means of control to track the MPP. This control is referred to as maximum power point tracking (MPPT). Several approaches to MPPT exist ranging from simple linear compensation to elaborate fuzzy and neural controllers [11]. For the purposes of this thesis, however, we simply assume that MPPT is present and ideal. Most converter manufacturers claim very high MPPT efficiencies. MPPT efficiency is the ratio of the power drawn by the converter and the actual maximum power of the panel. Published measurement results by Salas et al. also show high values, upto 99.9% [12].

The voltage and current of a single pV-module, about 30V and 8A at most [13], are relatively small compared to even domestic energy consumption. This being the case, modules are often connected in series to form so called strings whose voltage is at a more practical level, say 350V. These strings may then be connected in parallel to form arrays. Both interconnections have some issues which will be discussed next.

2.2 Behaviour of photovoltaic strings and arrays

When connecting photovoltaic panels in series there is always a risk of the panels not being in identical insolation conditions. Let us consider a string of two modules

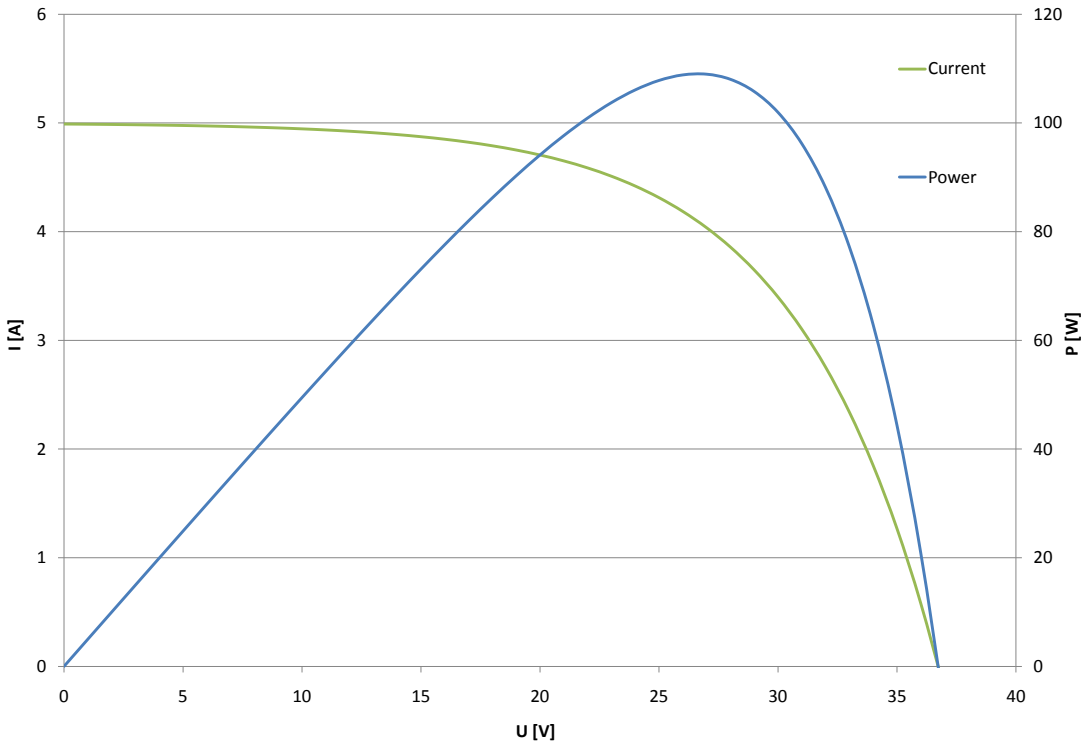

Figure 4: pV-module current and power as a function of voltage

in series, the other module shaded. Considering the equivalent circuit this situation would mean the current of one current source would decrease. The other module's current source would still force the current to be the same as before leading the diode in the first module to be forced into the reverse biased state of operation. Not being designed for such operation the pV-module would overheat and likely break [14]. To prevent this from occurring, pV-modules meant for series connection are equipped with bypass diodes, which start to conduct once the reverse bias reaches their forward drop voltage. The shaded panel will obviously not produce power, but neither will it brake.

The diode causes the current to rise steeply when there is negative voltage over the module. Assuming a stepwise rise makes it possible to derive the UI-curve of the string: it is simply a case of summing the voltage of the modules at each current point. An example is provided in Figure 5 with the power also included. This reasoning applies for any number of modules connected in series.

The power curve in Figure 5 poses a challenge for the MPPT: there are more than one local maxima. The challenge is to distinguish between local and global maxima without interrupting the flow of power. In this case most algorithms would find the maximum depending on where they start looking from. Starting at the short circuit current would yield a maximum at the lower voltage level while an open circuit voltage based approach would lead to the maximum at the higher voltage level. Algorithms that are more likely to find the global maximum also exist. One such

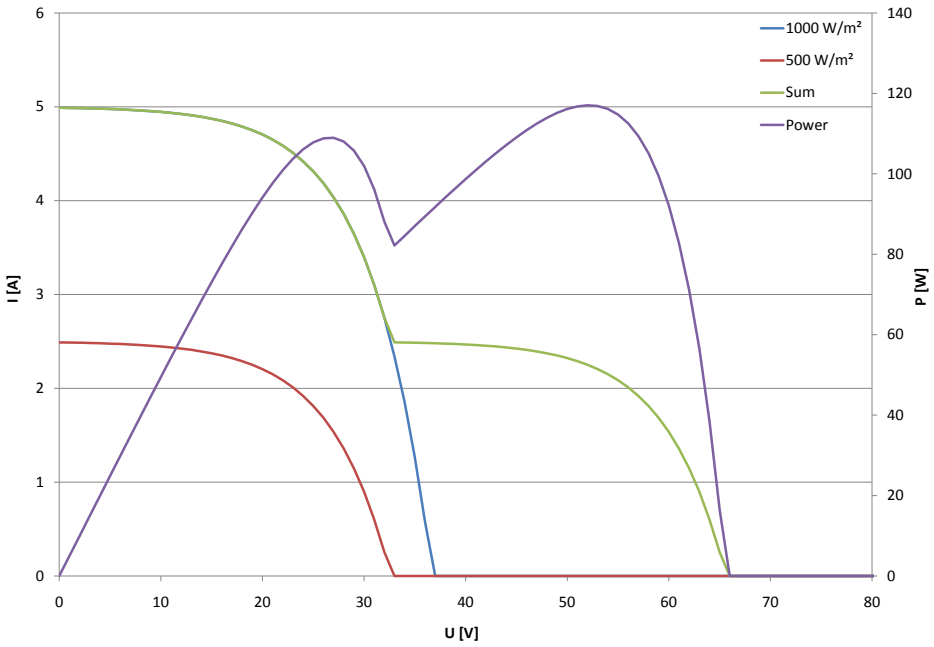

Figure 5: pV-string current and power as a function of voltage

MPPT method is described in [15]. The method is based on a priori knowledge of where the maxima are likely to be, such knowledge could be obtained by performing initialization sweeps or user input. In the case depicted in Figure 5 there would not be much difference power wise, but in other kinds of scenarios the maxima can differ significantly.

PV-modules or strings may also be connected in parallel to form arrays. In this case the voltage over the panels or strings will be the same. The voltage at which the array will operate is controlled by the MPP tracker of the power converter based on the power output of the array. The UI-curve of the array is similar to that of a string. In this case it is the currents of the modules that are summed at each voltage point. It is possible for the paralleled modules or strings to have different open circuit voltages, which would lead to one or several of them to not operate at their MPP. To prevent negative currents in the strings, they should be equipped with series diodes, often referred to as string diodes. If modules are connected directly in parallel, the series diode should be connected to the module. The UI and UP-curves of such a scenario are presented in Figure 6.

Figure 6 shows that the power has local maxima similar to the situation where a module in a string was producing less current. In this figure the local maximum at the higher voltage is clearly not a global maximum, a challenge again for the MPPT-algorithm.

The situation becomes more complex in a large installation, where modules will be connected in strings to provide a high voltage for optimal DC/AC-conversion and a large current to supply large central converters. Both of the above situations will occur simultaneously. The process of combing the above cases yields Figure 7,

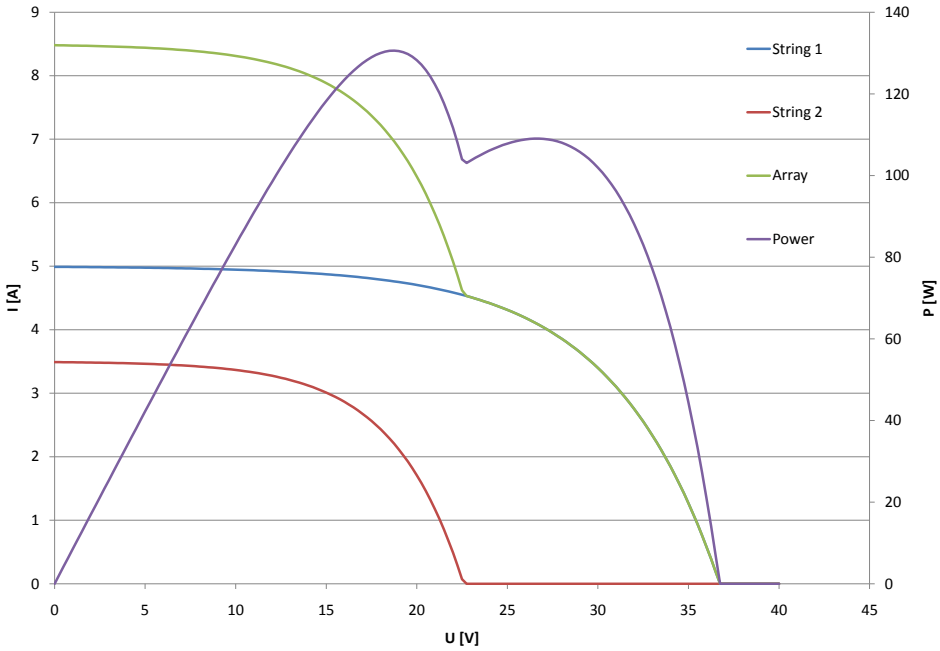

Figure 6: pV-array current and power as a function of voltage

which shows the UI-curve of an array of four modules, comprising two paralleled strings each with two series connected modules.

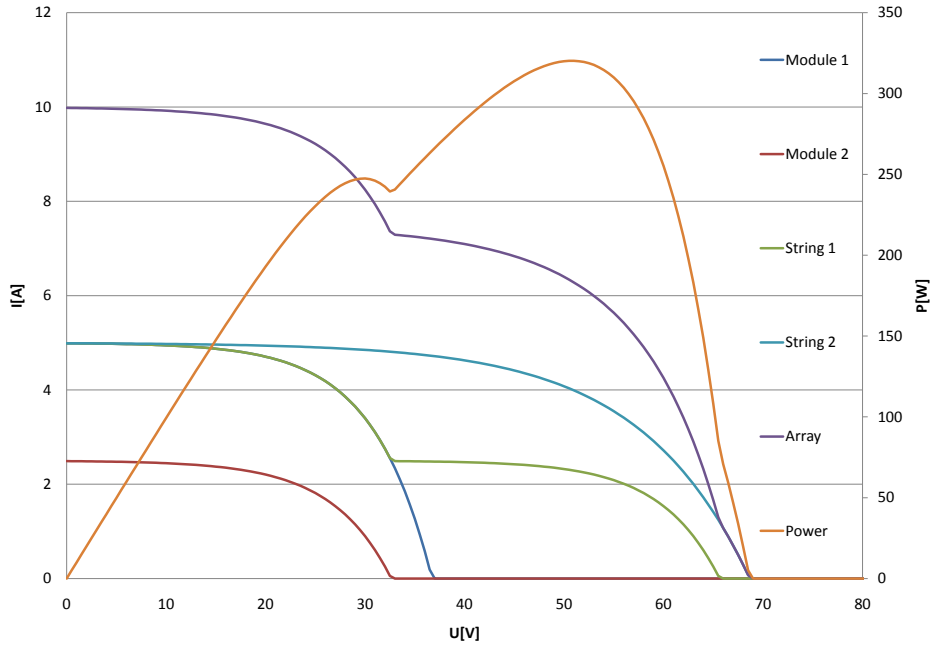

Figure 7: pV-array current and power as a function of voltage

Based on Figure 7 it would appear that the partial shading of one out of four panels does not have a very significant effect on the shape of the power curve. The curve is so similar to that of the single module shown in Figure 4, that even a simple MPP tracker would be likely to find the global maximum and thus give satisfactory power output. However, one string out of four, 25% of the panel area, would not be operating at its MPP. This might lead to significant losses in energy production over time, depending on the level of shading.

Transients in insolation will of course appear as day breaks, clouds pass, and the sun sets. These transients can be assumed to have little effect on the energy yield of the whole system, since they present themselves at times when insolation is small anyway, with the exception of a passing cumulus on a hot day. The effect of transients is neglected in this thesis and we concentrate exclusively on steady state systems.

2.3 Possible inverter configurations

There are several different ways to connect pV-panels to the AC-grid. The basic principles of three plausible configurations along with their known advantages and disadvantages are described in this section. These configurations include the so-called central inverter with or without a grid transformer, and variants of an inverter with added DC-boost conversion. The topologies have been reviewed by Kjaer et al. [16] and Huang et al. [17].

Central inverter

The simplest way to connect pV-power to the AC-grid is to connect 20–25 modules in series, in order to reach the voltage level of 625V needed to produce the AC-voltage of a 400V low-voltage grid, and connect them to the DC-side of a full-bridge inverter. Detailed calculations will follow next. Such a configuration is illustrated in Figure 8.

The DC-voltage level required to produce the voltage of the 3-phase AC-grid is the peak value of the line to line voltage divided by the modulation index. The maximum modulation index M for the most commonly used modulation methods, the space vector pulse width modulation (PWM) and carrier based PWM with the suboscillation method, is 0.907 [18, p. 157-161]. Increasing the modulation index beyond this value would require overmodulation [19, p. 210]. This would cause harmonics in the output voltage, which would have to be filtered out at a cost in efficiency. The needed DC-voltage can be calculated from

$$U_{DC} = \frac{\sqrt{2}U_{LL}}{M} \ , \tag{7}$$

where

$$U_{LL} = \text{ The line to line voltage of the AC-grid.} \tag{8}$$

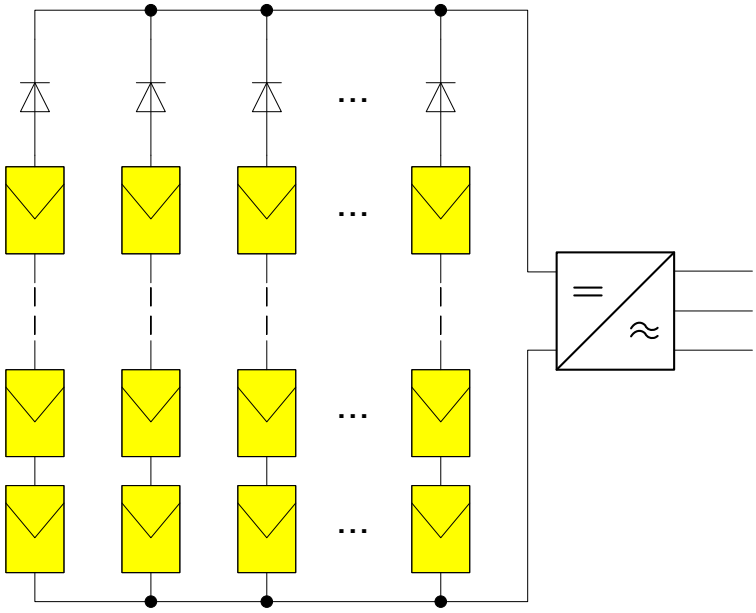

Figure 8: A pV-array with a central inverter

In Europe the required DC-voltage level would thus be

$$U_{DC} = \frac{\sqrt{2} \cdot 400V}{0.907} \approx 623V \ . \tag{9}$$

Hence enough panels have to be connected in series to reach 623V even on the hottest days of operation. Let as assume that the panel temperature on a sunny summer day would be 70°C. Let us take an example: according to its data-sheet, the 230W pV-module BP 3230T from BP Solar [2] has an MPP-voltage of 25.9V at NOC and a K_V of -0.36%/°C. The panel temperature at NOC is said to be 47°C. By inserting these values into (5), the panel's MPP-voltage at 70°C can now be found to be

$$U_{MPP} \ = 25.9V \cdot \left[1 + (70 - 47)^\circ C \cdot (-0.0036 \tfrac{1}{^\circ C})\right] = 23.76V \ . \tag{10}$$

Therefore, at least 27 modules would have to be connected in series to reach 623V.

The open circuit voltage of this module at NOC is 33.4V. Thus the open circuit voltage of the whole string at -20°C would be

$$\begin{aligned} U_{OC} \ &= 27 \cdot 33.4V \cdot \left[1 + (-20 - 47)^\circ C \cdot (-0.0036 \tfrac{1}{^\circ C})\right] \\ &= 1120V \ . \end{aligned} \tag{11}$$

This exceeds the 1000V limit specified by many panel manufacturers as the maximum DC-voltage of the system. Standard IEC 60364-7-712 [20] specifies the maximum DC-voltage of a pV-installation to be the voltage measured at STC, in other words 1000 W/m^2 insolation and 25°C. The open circuit voltage of the previous example string at STC would be

$$U_{OC} \ = 27 \cdot 36.7V \approx 990V \tag{12}$$

leaving very little headroom for manufacturing tolerances and other irregularities.

The logical conclusion is that the single stage inverter is inconvenient as such in a 3-phase AC-system at these voltage levels, especially if large temperature differences are to be expected. However, in North America, where the line to line voltage is only 208V in 3-phase and 240V in 2-phase systems, this configuration might well be viable. Other options are to use a step-up transformer on the grid side or use three single phase inverters. The first requires expensive and heavy grid frequency transformers, which make the inverter bulky in comparison to transformer-less inverters, that can be installed by a single electrician. The latter calls for at least twice the number of semiconductors, which increases the cost.

Inverter with central DC-boosting

A slightly more complex way to connect pV-panels to the AC-grid is to connect some panels in series and use a DC-boost converter to boost the voltage for the inverter. This way the boost converter can make sure that the panel system is at its MPP and that the inverter is fed a high enough voltage. Still, enough panels should be connected in series to make the efficiency of the boost conversion as high as possible. The principle is depicted in Figure 9.

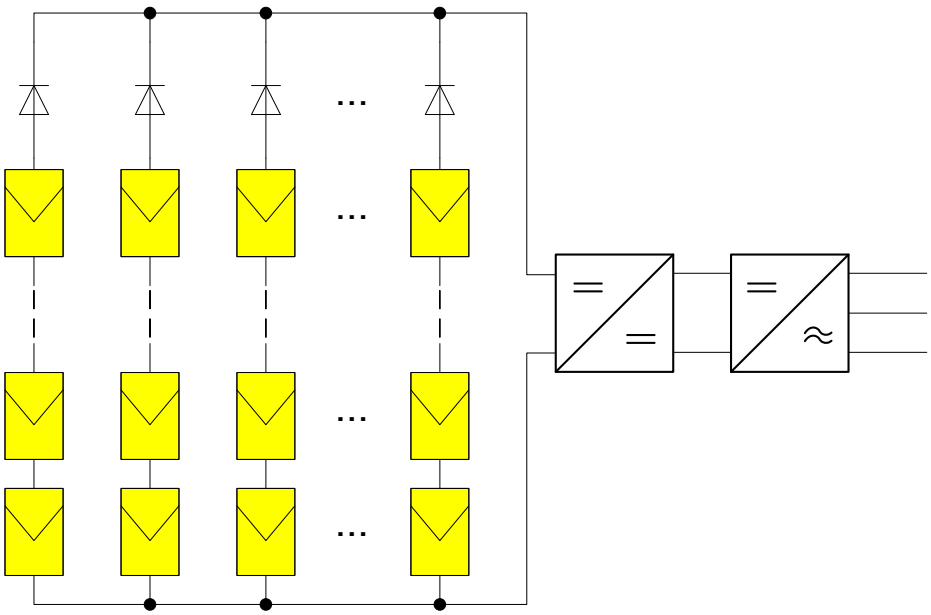

Figure 9: A pV-array with a central boost converter

This method has some advantages over the previously described single stage inverter. Mainly, a high enough DC-voltage can be produced for the inverter to function at the MPP of the installation with high efficiency and good power quality. This can be done without exceeding the voltage limits at the terminals of the panel installation.

Inverter with string boost converters

The use of boost converters also allows for greater modularity: several boost converters can be used to feed one inverter. If MPP-tracking is implemented in the boost converters rather than the inverter, fewer panels will be tracked by each converter leading to more precise tracking. A diagram of an installation with string boost converters is presented in Figure 10

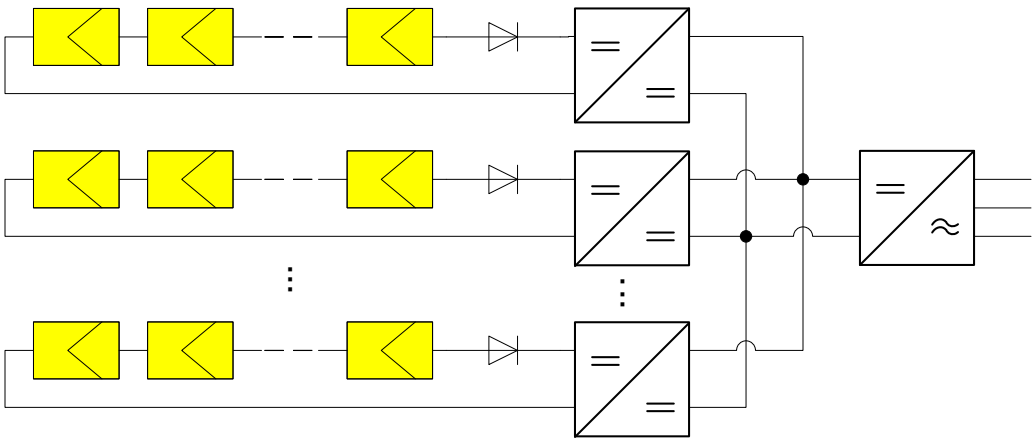

Figure 10: A pV-array with string boost converters

Partial shading or dirt problems can have a significant effect on energy harvesting in large installations. If the boost converters are positioned close to the panels, transmission lines can also be made with high voltages, which reduces losses from cable resistance.

The downside of using DC-boost converters is the loss in efficiency introduced by an added converter stage. Measurements by Matti Liukkonen at Aalto University School of Technology (currently Aalto University School of Electrical Engineering), department of electrical engineering from 2009 [21] show efficiencies of up to 97% for a 100kW boost converter. This is a decent efficiency for a DC-boost converter. However, market leaders in solar inverter technology are claiming 98% efficiencies for whole inverter systems [22]. An inverter with string boosting, although more efficient in harvesting energy in unbalanced installations, seems thus less attractive to buyers because of its smaller efficiency in optimal conditions.

Module inverter

The most extreme modularity in a pV-installation can be achieved with the so called module inverters. These devices are designed to handle the power of a single pV-panel, or module, as the industry likes to call them. The principle is presented in Figure 11.

A module inverter will operate at power levels of one or two hundred watts and input voltage levels of 20 to 40 volts at the input of the device. Therefore, the voltage has to be boosted at least tenfold to reach the levels needed for even a single phase European grid, or two or three phase North-American grids.

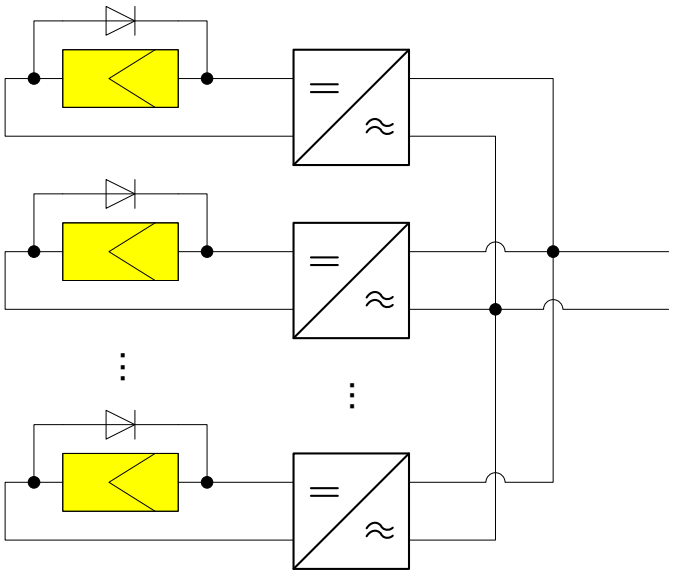

Figure 11: Module inverters

Their small power means a large number of devices are needed for even a moderately sized plant. The efficiency of the DC-DC conversion is also reduced at high conversion ratios typical for these devices. On the other hand, MPP-tracking is done at panel level ensuring optimal energy harvesting.

Module inverters are popular in residential rooftop installations, where installation sizes are relatively small and partial shading caused by trees and neighbouring houses is inevitable. The installation is also simple, since the devices need only be connected to regular wall sockets.

Galvanic isolation

In the USA, the National electrical code (NEC) dictates that one of the terminals of a pV-panel system has to be grounded [23]. Also the star point of the low voltage AC-grid to which the power is to be transmitted is grounded. Since neither of the DC-side terminals of a full-bridge inverter can be at the same potential as the star point or neutral of the connected AC-grid, grounding both sides of the inverter would lead to a short circuit through ground and the inverter would not function properly [16].

To avoid such a short circuit, the DC-side and the AC-grid must be galvanically isolated. This means using a transformer, which can be either a traditional grid frequency transformer or a more modern high frequency transformer. The latter would be connected on the DC-side of the inverter. The output of the pV-panel installation or the DC-boost converter would be fed to a high frequency chopper, isolated with a high frequency transformer, then rectified again. The output of the rectifier would thus be isolated from the panel installation and could be left to float. The principle is depicted in Figure 12. [16]

Both of the above methods have their advantages and disadvantages. A grid

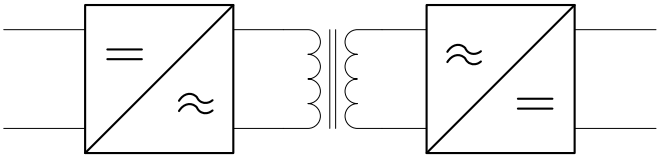

Figure 12: High frequency isolation principle

frequency transformer of even 20kW would be heavy and expensive, but the technology is tried and mature. The size of a transformer is approximately inversely proportional to its operating frequency so a high frequency transformer would be considerably smaller and thus cheaper. However, the high frequency solution would consist of an extra chopper and rectifier, neither of which would be 100% efficient.

Both isolation configurations have one added benefit: the possibility to step-up the voltage. This would make it possible to use a smaller DC-voltage to connect to the grid without using a boost converter. This is in fact how the 3-phase solar inverters tested in Section 2.4 operate, they have a DC-bus voltage of around 450V from which the inverter produces an approximately 320 volt line to line AC current. The current is fed to a 3-phase step-up transformer that raises the voltage to 400V.

2.4 Inverter comparison and measurement results

Solar inverter manufacturers claim very high efficiencies for their devices. The German manufacturer SMA (SMA Solar Technology AG, Niestetal, Germany) for example claim efficiencies up to 98%, for their SUNNY MINI Central models [22]. This is such a high claim, that we wished to verify it for ourselves. We tested the single phase 9kW model Sunny Mini Central 9000TL-10 and, to get a better understanding of the solar inverters on the market, also two 3-phase models from other manufacturers, the Spanish 20 kW Global Inver Sonne Sn20 (Global Sonne, Sant Fruitós de Bages, Spain), and the Chinese 10kW Sungrow SG10K3 (Sungrow Power Supply Co. Ltd, Hefei, Anhui, China).

The SMA inverter is a single phase device so its theoretical minimal input DC-voltage would be the amplitude of the phase voltage of the 230V grid, namely 325V. The installation guide of the device states an MPP range of 333V to 500V. The other two devices are 3-phase and have step-up transformers on the AC-side allowing for a DC-voltage range of 450V to 700V and 450V to 500V, for the Sn20 and SG10K3 respectively.

SMA provides the efficiency as a function of output power. Acquiring similar measurement data was a logical aim for these measurements, since the objective was indeed to confirm the manufacturers' claims.

The measurements were performed in January 2010 at the Aalto University School of Technology, Department of Electrical (currently Aalto University School of Electrical engineering). Actual pV-panels where replaced with a DC-voltage source consisting of a three-phase variac, six-pulse diode bridge, a 6mF capacitor pack, and a high power resistor network. The variac provided the ability to adjust the DC-voltage level. The capacitors were used to smooth the voltage ripple from the

six-pulse bridge.

All solar inverters have some kind of MPP-tracker. Its purpose is to find the operating point at which the source outputs the most power. Since the pV-panel provides a DC-source, this involves finding the operating point at which the product of voltage and current peaks. To produce such an operating point a resistor was connected in series with the voltage source. The circuit diagram of the measurement set-up is presented in Figure 13.

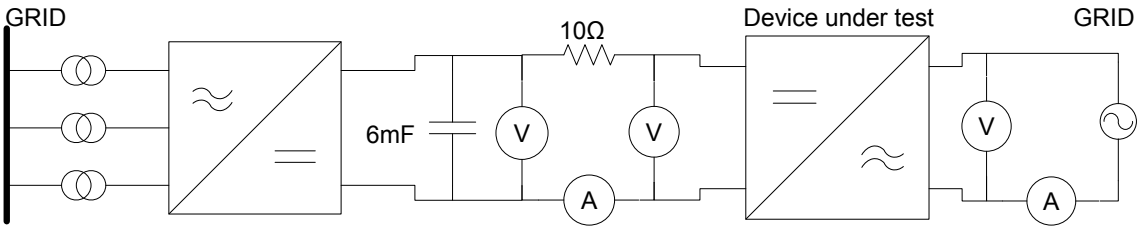

Figure 13: Circuit diagram of the efficiency measurement set-up

The voltages and currents where measured with a Voltech PM6000 six-channel power analyser (Voltech Instruments, Inc. Fort Myers, Florida, USA) and Danfysik Ultrastab 867-2001 current transducers (LEM Danfysik A/S, Smørum, Denmark). The efficiency was first calculated in the normal manner as

$$\eta = \frac{P_{out}}{P_{in}} \ . \tag{13}$$

This calculation, however, led to values of efficiency spiking over 100%. Since it not possible for a device to have an efficiency of over 100%, it was concluded that the reactive components in the inverter acted as energy storage and caused the ratio of the output and input power to momentarily exceed one. To get rid of this problem, the efficiency was then calculated as

$$\eta = \frac{W_{out}}{W_{in}} \ , \tag{14}$$

where

$$W_x = \int_0^{6s} P_x \mathrm{d}t \ . \tag{15}$$

The weakness of the measurement set-up is that the input voltage and current of the inverter cannot be independently controlled. The voltage over the capacitor could be adjusted so that the voltage at the input of the inverter reached the desired value, but the current would then be defined by the inverter MPP tracker based on the value of the series resistor. Figure 14 shows the current and power of the inverter as a function of voltage assuming ideal MPP-tracking with a 10Ω series resistor.

It can be seen from Figure 14 that the maximum of the power is at half of the open circuit voltage. At this point the input impedance of the inverter is

$$Z = \frac{u}{i} = \frac{15\mathrm{V}}{1.5\mathrm{A}} = 10\Omega \ , \tag{16}$$

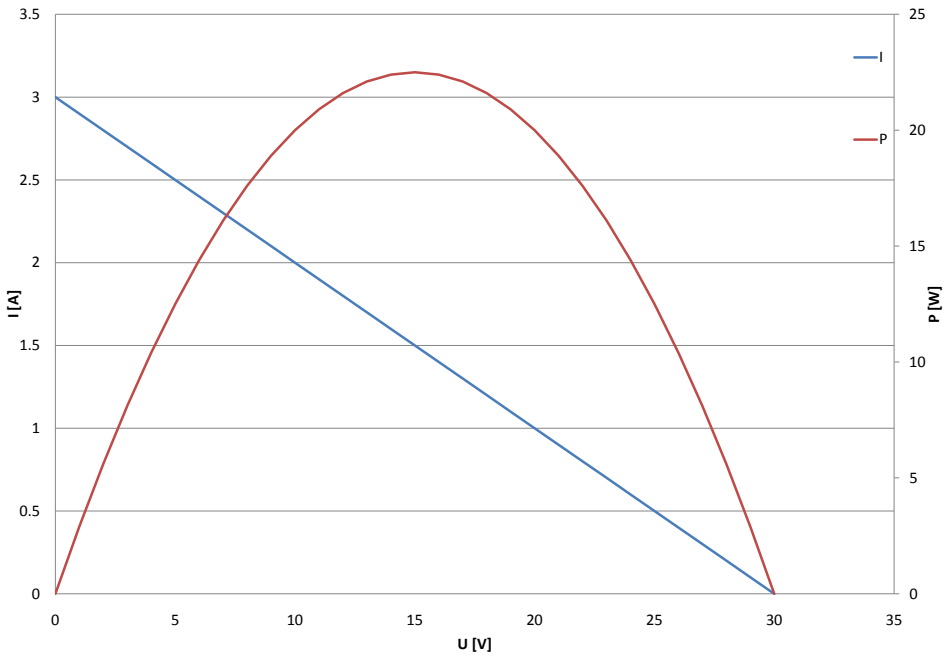

Figure 14: Inverter power and current as a function of voltage

which is the same as the value of the series resistor. This is as basic circuit theory would suggest. Due to this behaviour, relatively high DC-voltages had to be provided in order to keep the MPP-voltage in the operating range of the inverters. Also protective circuitry had to be installed to prevent the inverters from being exposed to the full open circuit voltage of the voltage source. This would have occurred if the inverter had stopped drawing current through the resistor.

It turned out that the high power resistor network used as the series resistance caused the DC-source to be coupled to ground. The coupling was not documented so it was concluded that it was parasitic coupling through the 3-phase ventilation fan motor. Nevertheless, the tested inverters detected this coupling as a ground fault and would not operate. An additional isolation transformer had to be introduced to isolate the resistor auxiliary power supply from the grid.

The three solar inverters where measured using the measurement set-up described above. The exact measurements documented in the manual of the SMA device could not be replicated due to the shortcomings of our power supply, but a good estimate of the efficiency level could still be determined. The change in efficiency as a function of DC-voltage should be less than 0.5% according to the manual [22].

The efficiency of the grid frequency transformer of the Global Inver Sonne device was also measured. This measurement was of more use since the voltage at the transformer input was regulated by the inverter. The inverter measurement results are presented in Figure 15. The Global Inver Sonne transformer efficiency is presented in Figure 16.

The measured efficiency of the SMA inverter was very high, peaking at 97.7%

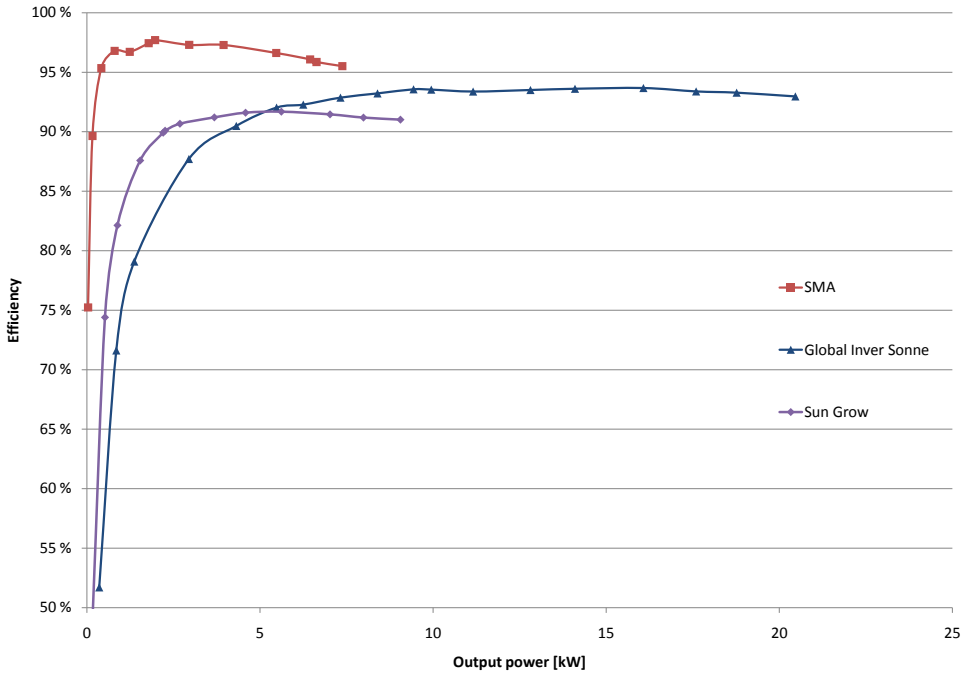

Figure 15: Inverter efficiency as a function of output power

at 2kW output power. The decreasing of the efficiency at higher power levels would suggest that the bulk of the losses at high power are conduction losses in the power semiconductors rather than the auxiliary circuitry. The rapid rise of the efficiency at low power corroborates this finding and shows that the auxiliary circuitry consumes very little power. The shape of the measured curve is almost exactly matches the one found in the SMA installation guide [22].

The Global Inver Sonne measurement results show reasonable efficiencies for the inverter on its own, but when the transformer is added, the total efficiency falls significantly behind that of the SMA device. The Sn20 would appear to have a larger auxiliary power consumption and the 90 % efficiency level is only reached at 20 % power or more, while the SMA inverter efficiency peaked at only 22% power. Coupled with the transformers suboptimal performance at low power levels, the total efficiency at power levels under 50 % leave something to be desired.

The measurements for the Sungrow SG10K3 show results similar to those of the Global Inver Sonne Sn20. The curve is almost identical when the powers are scaled, but the efficiency is a few percentage units lower. On an absolute scale the efficiency at low power is higher, which is only natural since the device is designed for half the power. Transformers are a mature product, whose efficiency is mostly affected by power level. It is therefore reasonable to assume that most of the losses in this inverter's case are introduced by the actual semiconductors and their auxiliary circuitry.

As a side note it is worthwhile to note the weights of the three inverters tested. According to their manual the devices' weights are 35kg for the SMA, 300kg for the Global Inver Sonne, and 175kg for the Sungrow device. As a reminder, the rated

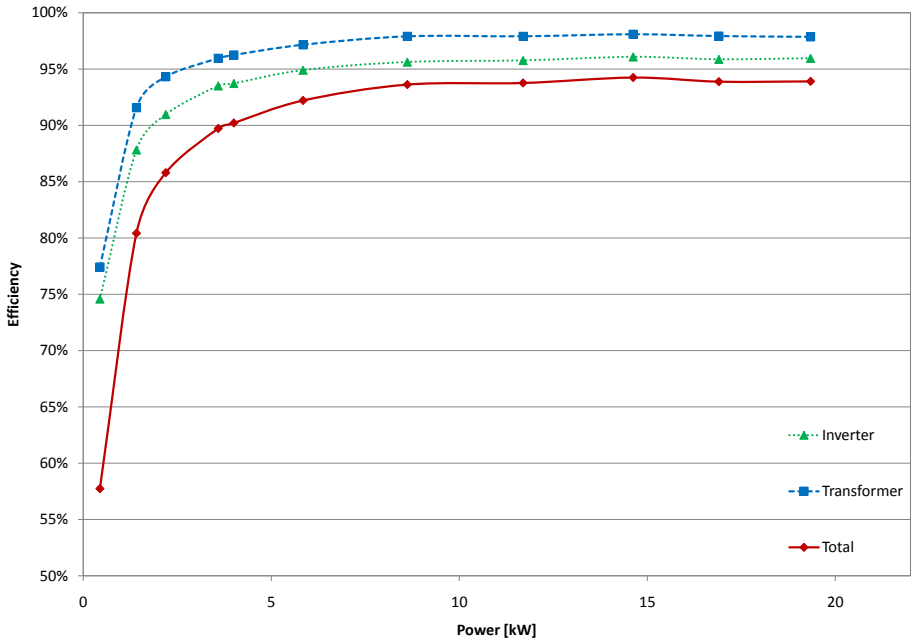

Figure 16: Global Inver Sonne Sn20 inverter and transformer efficiency as a function of output power

output powers of the inverters were 9kW, 20kW and 10kW respectively.

The efficiency measurements on the whole gave the expected results. The results show that there are significant differences between the devices, even the Sungrow and Global Inver Sonne devices, which have the same configuration. The results also agree with the specifications of the manufacturers, which would indicate that the measurement set-up is viable and could be used in prototyping to give at least preliminary efficiency results.

3 Solar plant energy yield calculation

The main focus of this thesis is the development of a tool to calculate the possible energy yields of different inverter configurations under known insolation and temperature conditions. In the previous sections it has been established that the MPP-current of a solar panel mostly depends on the insolation and the MPP-voltage depends on temperature. With the further assumption that the solar installation is always operated at the MPP, the plant energy as a function of time can be formulated as

$$E(t) = \int_0^t U_{MPP}(T)\, I_{MPP}(S) \prod_{m=1}^{n} \eta_m \left[U_{MPP}(T)\,; I_{MPP}(S)\right] dt, \tag{17}$$

where

$\eta_m[U, I]$ = the efficiency of converter stage m as a function of current and voltage
n = the number of cascaded stages
T = temperature as a function of time
S = insolation as a function of time

The first term is a simple integration of electrical power, the product of DC-voltage and current. The second term, the product of the stage efficiencies, is based on the definition of the efficiency of cascaded power stages. The efficiency of each stage depends on the input voltage and current of the stage. For simplicity, the voltage is assumed to be temperature dependant and the current insolation dependant.

Time frames up to one year should be evaluated in order to get a reliable picture of the energy yields. This means large amounts of data, thus forcing the use of a computer to evaluate the energy. One of the initial goals was to use readily available software for the evaluation. Scientific software such as Matlab, while powerful, are expensive and are not very attractive to the target group of the tool, salesmen and executives. Therefore, the tool was implemented using Microsoft Excel (Microsoft Corporation, Redmond, WA, USA), a spreadsheet calculation program found in most offices around the world. Matlab was used to confirm the validity of the spreadsheet tool with more accurate models.

Because Excel was used and, more importantly, insolation and efficiency data are not continuous, but discrete, the energy equation was discretized. The plant energy becomes

$$E(h) = \sum_{k=0}^{h} U_{MPP}(T(k))\, I_{MPP}(S(k)) \prod_{m=1}^{n} \hat{\eta}_m \left[U_{MPP}(T(k))\,; I_{MPP}(S(k))\right]. \tag{18}$$

In most cases, there will be at least two cascaded stages: the inverter stage and a step-up stage. The step-up stage can be either a DC-DC boost converter between the panel installation and the inverter or a transformer between the inverter and the grid.

To calculate the energy, the unknown values in (18) have to be evaluated. The evaluation is done numerically based on tabled values, approximate models, and interpolation. The voltage and current are evaluated based on an approximate model of the pV-array and tabled insolation and temperature values. The efficiencies are interpolated from measured efficiency tables. The approximate model, the evaluation of the system MPP, and the interpolation method are discussed in this section. A flowchart illustrating the process of calculating the the energy output of an installation with measured insolation and temperature data is shown in Figure 17.

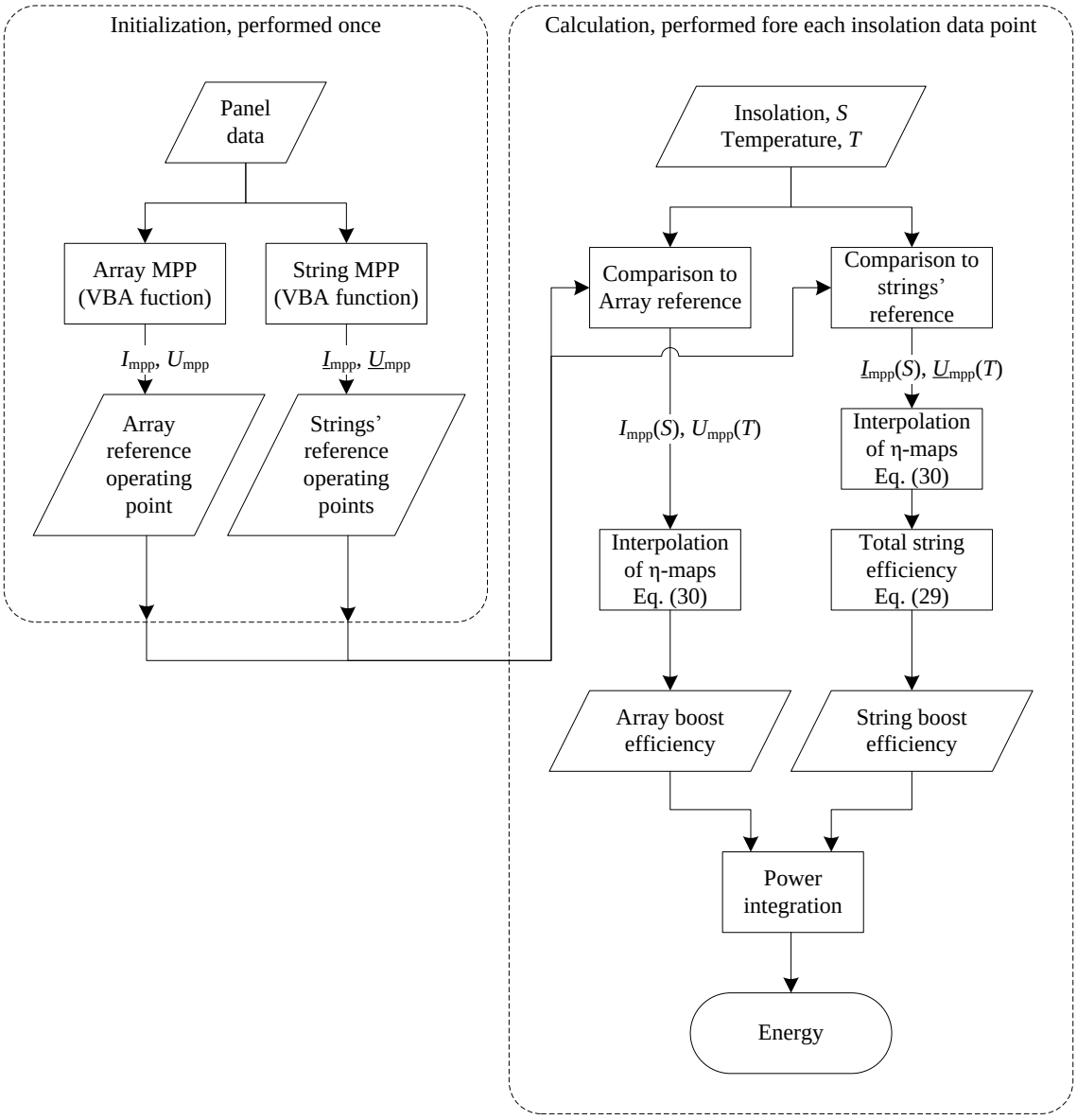

Figure 17: Flowchart of the Excel calculation tool

3.1 An approximated pV-model

When making calculations based on a large amount of data, a compromise has to be made between speed and accuracy. Excel can only perform simple calculations on large amounts of data. Our analysis was based on 8760 rows of data, which proved to be a large amount for Excel. Complex calculations on such an amount of data caused the program to crash or led to calculation times in excess of five minutes. Since the aim is to produce a tool that can be used to compare inverter configurations on the fly, calculation times had to be reduced to less than a minute.

The most significant approximation was made in the model of the photovoltaic cell. Instead of using the mathematical model given in Equation (3), a cruder piecewise linear model was used. The exponential curve was replaced by two strait lines connecting the short circuit current, MPP- voltage and current, and open circuit voltage. Figure 18 illustrates the approximation. The approximation makes the calculation of string and array MPP much simpler.

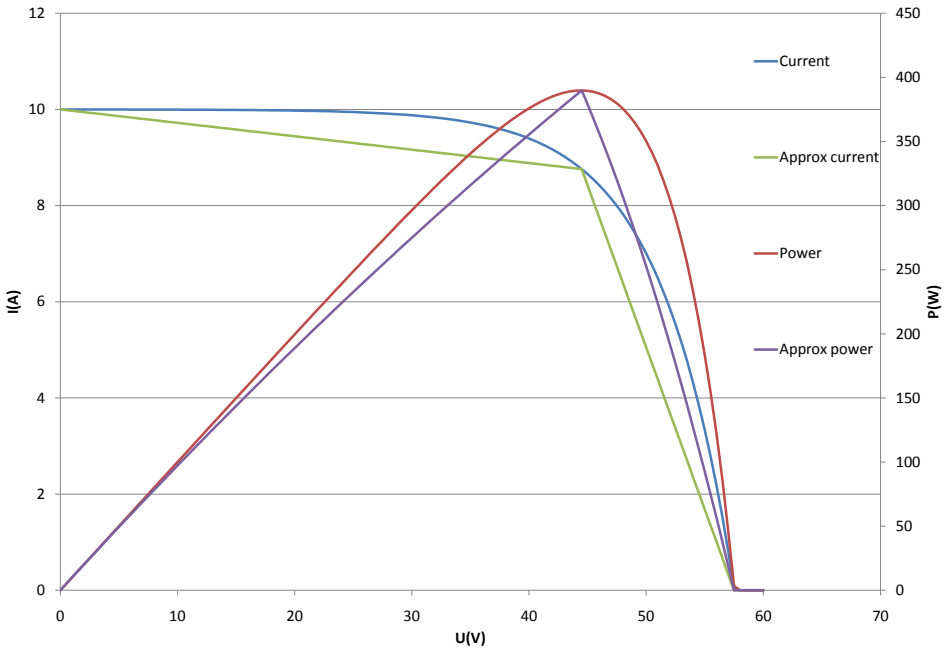

Figure 18: Inverter power and current as a function of voltage

In normal operation, pV-panels are operated as close as possible to the MPP. As a result, the above approximation is satisfactory most of the time. The approximation only becomes inaccurate when a panel is forced out of its MPP. This would happen, for example, if the MPP voltage of several strings connected to a central inverter would differ significantly. The nature of the approximation is such that the calculation will always yield slightly inferior performance in comparison to the more exact mathematical model.

3.2 Evaluation of the installation MPP

The calculator compares three inverter configurations, one with string specific boost converters with built in MPPT connected to a central inverter, one with a centralized boost converter connected to an inverter, and one with a centralized inverter connected to a grid frequency transformer. For the purpose of this analysis it was reasonable to assume that the MPPT implementation in the various power electronic converters is ideal, i.e. the converters always operate at the global maximum power point of the connected panel system.

Some custom Excel functions were implemented with Microsoft's Visual Basic for Applications (VBA) to cover the calculation needs posed by the different configurations. These functions will be described in the following paragraphs.

Let us first consider an installation with string specific boost converters. In this kind of installation, the MPPT would be implemented in the boost converter. Each string would thus operate at its MPP, which depends on the parameters, shading, manufacturing tolerances, dirt, insolation, and temperature of the connected panels. The first objective is to find this MPP based on these conditions. The shading and dirt have the same effect so they are combined and given as a single percentage for each individual panel in a column where cells correspond to individual panels. Manufacturing tolerances are given in the same manner and panel parameters are presented in a separate column. Insolation and temperature are presented in two columns where they can be imported from a database of choice.

The temperature provided in databases is the generally ambient temperature. The temperature of the actual panel depends strongly on insolation and installation. Insolation causes the panel to heat above the ambient temperature, but the rise can be alleviated by installing the panels so that wind and convection allow for some degree of cooling. A temperature rise factor can be input by the user as degrees per kW, depending on what degree of temperature rise is to be expected. This rise factor describes how much warmer the panel is compared to ambient temperature as a function of insolation. The actual panel temperature is calculated for each data point to be used for further calculations.

To find the MPP of the string, an algorithm is used to calculate the its characteristic curve based on the panels connected to it and their operating conditions. The resulting curve is a piecewise linear plot whose corner points can be calculated based on the data for the panels and the temperature and insolation conditions. The algorithm then assumes that the MPP must be situated in one of these corner points.

The power curves are not piecewise linear, but piecewise quadratic. Furthermore, the sections open downwards, so they could theoretically have a maximum at the zero-crossing point of their derivative in addition to the corner points of the voltage-current curve.

If the voltage is less than the MPP-voltage, the current and power will be

$$I(U) = \frac{I_{MPP} - I_{SC}}{U_{MPP}} U + I_{SC} \tag{19}$$

$$\Leftrightarrow P(U) = \frac{I_{MPP} - I_{SC}}{U_{MPP}} U^2 + I_{SC} U \tag{20}$$

Let us now take the derivative with respect to U in order to find the maximum.

$$\Rightarrow \frac{dP(U)}{dU} = 2 \cdot \frac{I_{MPP} - I_{SC}}{U_{MPP}} U + I_{SC} \qquad = 0 \;\; ||I_{MPP} = x I_{SC} \tag{21}$$

$$\Leftrightarrow U = \frac{U_{MPP}}{2(1-x)}. \tag{22}$$

$$\lim_{x \to 1} U = \infty. \tag{23}$$

The infinite limit in (23) when the ratio x between the MPP-current and short circuit current approaches 1 simply means that if the current is constant with respect to voltage, the maximum power will be achieved at an infinitely large voltage. The ratio is typically 0.9 [24]. To be on the safe side, let us choose $x = 0.8$ for our calculation:

$$U = \frac{U_{MPP}}{2(1-0.8)} = 2.5 \cdot U_{MPP}. \tag{24}$$

Choosing an x larger than 0.8 will lead to even larger values. It is safe to conclude that there is no local maximum between 0 and the MPP-voltage.

Let us continue with the case where the panel output voltage is between the MPP-voltage and the open circuit voltage. The current as a function of voltage will be

$$I(U) = \frac{-I_{MPP}}{U_{OC} - U_{MPP}} (U - U_{OC}) \tag{25}$$

$$\Leftrightarrow P(U) = \frac{-I_{MPP}}{U_{OC} - U_{MPP}} \left(U^2 - U \cdot U_{OC}\right) \tag{26}$$

$$\Rightarrow \frac{dP(U)}{dU} = \cdot \frac{-I_{MPP}}{U_{OC} - U_{MPP}} (2U - U_{OC}) = 0 \tag{27}$$

$$\Leftrightarrow U = \frac{U_{OC}}{2} < U_{MPP} \approx 0.8 \cdot U_{OC}. \tag{28}$$

The maximum would be smaller that the MPP-voltage, where this equation no longer applies, so we can conclude that there is no maxima between the MPP-voltage and the open circuit voltage either. It can now be concluded that the maxima have to be at the corner points. Therefore the algorithm in the function can find the global maximum power and the corresponding voltage and current by comparing the values at the corner points. The function returns the voltage or current depending on a parameter chosen by the user.

Another function was implemented to give similar functionality for an array of panels, i.e. several strings in parallel. An array specific power electronic converter

would operate at the MPP of the whole array, which depends not only on the MPPs of the paralleled string, but also on their power output. The shading and manufacturing tolerances are now provided in an array where each column corresponds to a string of panels. As before each cell in the columns represents an individual panel. The other data required is the same as in the string function to enable easy comparison between the configurations. The algorithm again first determines the shape of the characteristic curve of the array by calculating the corner points. Based on the same logic as in the previous case of a single string, the maxima can be found at the corner points of the piecewise linear characteristic curve. Again, the function returns either voltage or current, depending on a final parameter.

Figure 19 shows a plot of both current and power of an array and its individual strings illustrating how the MPP point is determined.

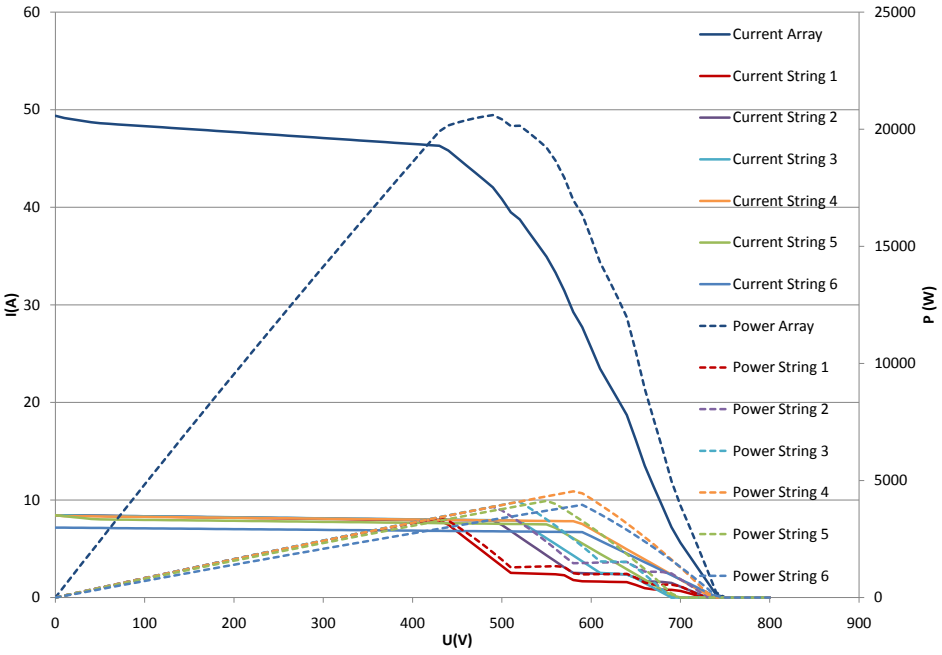

Figure 19: The current and power of an array and its individual strings as a function of voltage

3.3 Efficiency calculation

After the operating points of the panel systems have been determined, the next task is to interpolate the efficiencies of all the remaining system parts at that operating point. The efficiencies are given in two-dimensional maps and the function described in the next section is used for interpolation. The total efficiency of the system is simply the product of the efficiencies of the subsystems, except in the case of the string specific boost converters, where the total boost efficiency was calculated in

the following way.

$$\eta_{Boost} = \frac{P_{out}}{P_{in}} = \frac{\sum P_{out\,i}}{\sum P_{in\,i}} = \frac{\sum P_{in\,i}\eta_i}{\sum P_{in\,i}} \tag{29}$$

The ratios between MPP and open circuit voltage and MPP and short circuit current remain approximately constant regardless of insolation and temperature. On the other hand, the open circuit voltage depends linearly on temperature and short circuit current linearly on insolation. If we make two further assumptions, we arrive at a linear dependency between MPP-voltage and temperature, and MPP-current and insolation. We must assume that the effect temperature has on current is negligible and that the voltage remains constant as a function of insolation. The latter is strictly not true, voltage has a logarithmic dependency on insolation that can be solved from the mathematical model of the pV cell. However, the knee of the logarithmic curve is at roughly 100W/m^2 at which point next to no energy is produced, so it is a reasonable assumption that when producing energy, voltage is almost constant with respect to insolation. The dependence of current on temperature is defined as the temperature coefficient for current, a constant provided by panel manufacturers. This constant is usually two decades smaller than the corresponding constant for voltage, so we can conclude that both assumptions are reasonable in this case.

The linear dependencies derived above are of great use when calculating the energy produced by a pV system over a long period of time. It is time-consuming to calculate the operating point of a large array of panels or a large number of strings of panels, even with the linear approximation; the calculation of the MPP of the system used in Section 4 takes up to one second. If we use the linear dependencies above, it is enough to calculate the operating points once for a set of reference conditions and simply scale the results for all other conditions. This method allows calculation of the MPP for thousands of insolation-temperature pairs in a matter of seconds, instead of thousands of seconds.

The calculator was validated using a Matlab Simulink model. For this the Excel calculator was simplified to include only one panel. The temperature and insolation data of one day were fed to a Simulink model consisting of a pV-model based on the Shokley diode equation and an optimal MPP tracker. Both models yielded very similar results. Slight differences were caused by the fact that the Excel model does not account for the voltage's dependence on insolation; the total difference is about 1.25%. The validation data is available in Table A1 of Appendix 5.

3.4 Interpolation of efficiency maps

The efficiencies of the components of a solar plant are presented in two dimensional efficiency tables, the dimensions here being voltage and current. To approximate the efficiency at any given operating point, interpolation must be used. The nature of the calculations in this thesis is such that linear interpolation is the obvious choice. However, since the data is given in a two dimensional table, this interpolation has to be made in two dimensions. The definition of the bilinear interpolate that gives

an approximation of the efficiency with the given values of current i and voltage u is given below in Equation (30) [25].

$$\hat{\eta}(i,u) = (1-i_f)(1-u_f)A + i_f(1-u_f)B + (1-i_f)u_f C + i_f u_f D \ , \tag{30}$$

where

$$\begin{array}{ll} A = \eta(i_n, u_n) & B = \eta(i_{n+1}, u_n) \\ C = \eta(i_n, u_{n+1}) & D = \eta(i_{n+1}, u_{n+1}) \ , \end{array}$$

and

$$\begin{array}{lcl} i_n & = & \text{The largest tabled current value smaller than } i \\ u_n & = & \text{The largest tabled voltage value smaller than } u \\ i_{n+1} & = & \text{The smallest tabled current value larger than } i \\ u_{n+1} & = & \text{The smallest tabled voltage value larger than } u \\ i_f & = & \dfrac{i - i_n}{i_{n+1} - i_n} \\ u_f & = & \dfrac{u - u_n}{u_{n+1} - u_n} \ . \end{array}$$

Let us illustrate the interpolation with an example. A simple example of an efficiency table is presented in Table 1.

Table 1: Mock-up efficiency table

U \ I	0.5A	1A	3A	5A
5V	25%	31%	44%	60%
10V	47%	58%	77%	85%
15V	51%	73%	84%	91%

If we would like to approximate the efficiency of the system at 1.5A and 8V, we can now use the method described above. According to Table 1, the values A, B, C, and D would be

$$\begin{array}{llll} A & = 0.31, & B & = 0.44 \\ C & = 0.58, & D & = 0.77. \end{array}$$

The neighbouring current and voltage values would be

$$\begin{array}{llll} i_n & = 1A, & i_{n+1} & = 3A \\ u_n & = 5V, & u_{n+1} & = 10V. \end{array}$$

The fractional current and voltage would be

$$\begin{array}{lll} i_f & = \dfrac{1.5A - 1A}{3A - 1A} & = 0.25 \\ u_f & = \dfrac{8V - 5V}{10V - 5V} & = 0.6. \end{array}$$

By substituting the above into (30) we get

$$\begin{aligned}\hat{\eta}\left(1.5A; 8V\right) &= \left(1-0.25\right)\left(1-0.6\right)0.31 + 0.25\left(1-0.6\right)0.44 \\ &\quad + \left(1-0.25\right)0.6\cdot 0.58 + 0.25\cdot 0.6\cdot 0.77 \\ &= 0.5136 \approx 51\%.\end{aligned}$$

Considering the neighbouring values, 51% seems to be correct.

Unfortunately, Microsoft excel does not have a built-in function for bilinear interpolation. Thus an interpolation function had to be implemented. This was done using VBA, a language used to create functions and macros for use in Excel spreadsheets.

A screenshot of the Excel tool is presented in Figure 20.

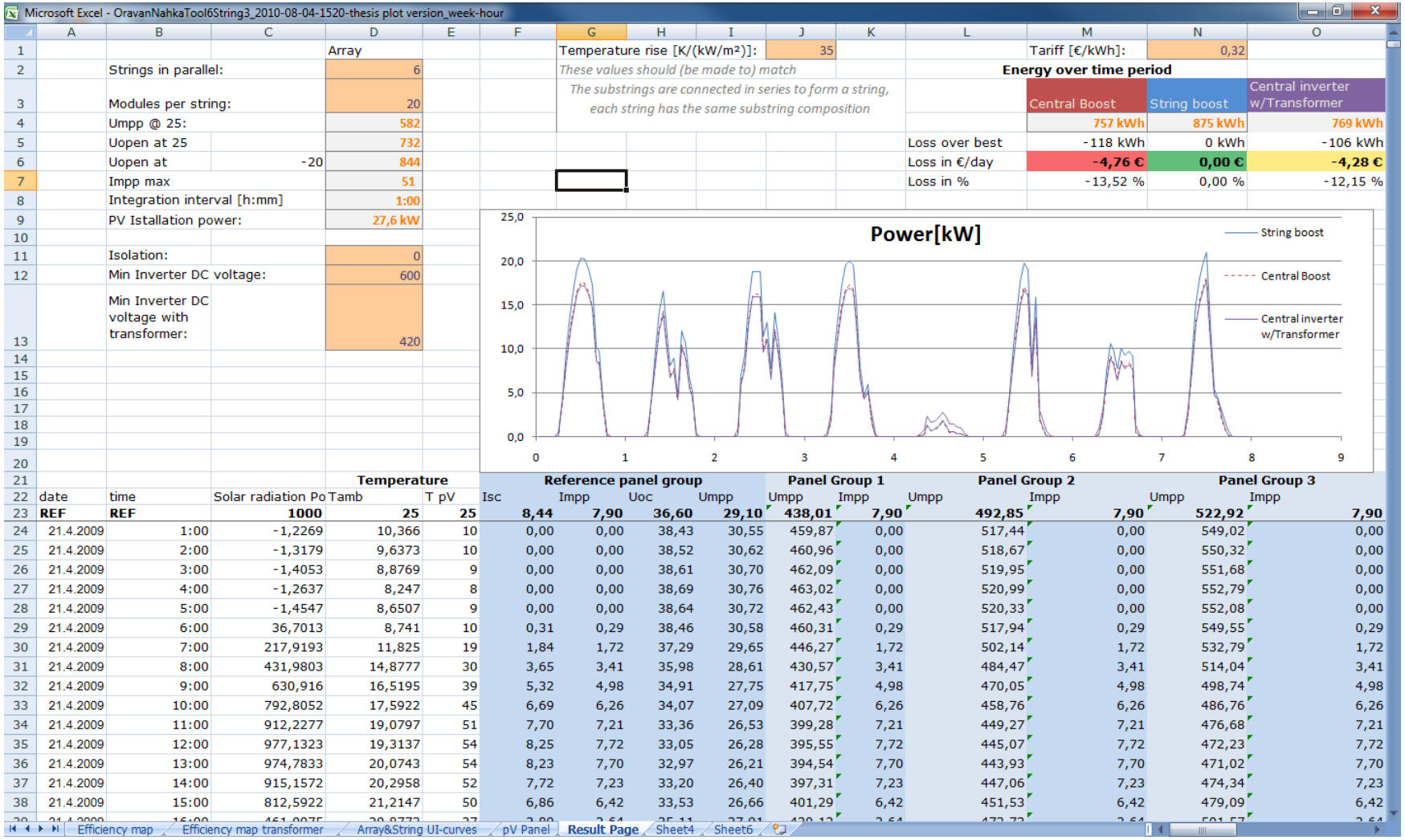

Figure 20: Screenshot of the Excel calculator

4 Results

4.1 Simulation results

The results of a comparison of pV system configurations done with the Excel calculation tool described previously are presented in the following section. The insolation and temperature data for the comparison were imported from the internet pages of the Solar Radiation Research Laboratory (SRRL) of the National Renewable Energy Laboratory (U.S. Department of Energy) [26]. SRRL keeps solar irradiation and various meteorological data on their Internet pages from the year 2001 with a resolution of one minute. Earlier data is also available but with fewer measurements.

The efficiency maps are based on the measurements described in Section 2.4, inverter manuals, and boost converter measurement data provided in [21]. The efficiency maps were scaled so that their rated power matched the power of the rest of the system.

Two pV systems were mainly compared, each consisting of six parallel strings of 20 panels each. The panel parameters are based on the 230W aleo S_18 solar module (aleo solar AG, Oldenburg, Germany) [13]. One of the systems had a boost converter for each string while the other one only had one boost converter for the whole array. Both systems were then connected to a grid inverter. A transformer configuration was also compared but the comparison is not totally fair, because a transformer system would be optimized for a different input voltage. In these measurements the inverter input voltage used for the transformer equipped system was 440V.

The first results show the performance of the different configurations when there is no mismatch between the panels and all panels are subject to the same insolation. The results are presented in Table 2 and Figure 21.

Table 2: Energy yield of different configurations over one year, one hour resolution, no shading

	Central Boost	String boost	Central inv. + Transf.
Energy	40851kWh	40851kWh	41176kWh
Loss over best	-325kWh	-325kWh	0kWh
Loss in %	-0.8%	-0.8%	0.0%

It can be seen from Table 2 that the central and string boost configurations yield exactly the same power and energy. This is as expected because the efficiency map of the boost converter has bean scaled to the power level of the converter, this means the efficiency depends on the ratio of rated power and actual power rather then absolute power. The inverter and low frequency transformer combination produces slightly more energy although it has a slightly worse efficiency at full power. The net efficiency of the different systems is plotted in Figure 22. Careful examination of Figure 22 shows that the transformer configuration has a better net efficiency at low power levels. This becomes even more evident in the later calculations.

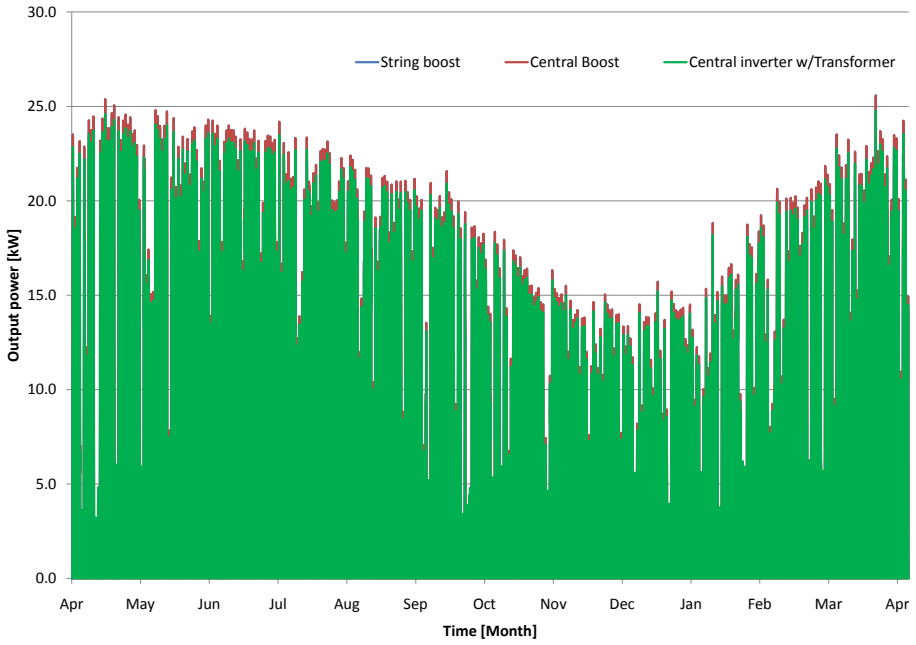

Figure 21: Plant output power as a function of time over a year, one hour resolution, no shading

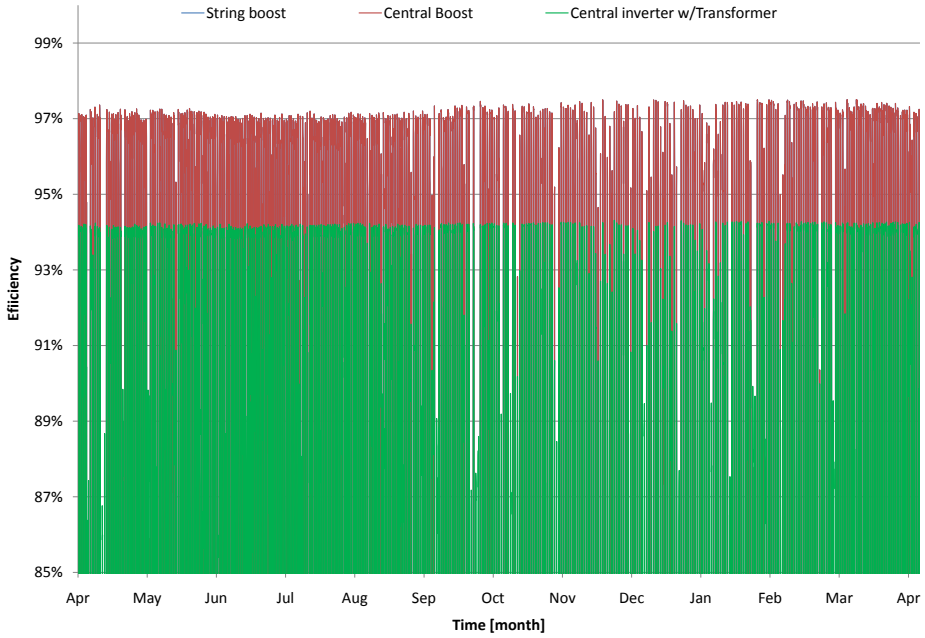

Figure 22: Plant efficiency as a function of time over a year, one hour resolution, no shading

Table 3: Panel array shading percentages used in the calculation

panel \ string	1	2	3	4	5	6
1	0.0%	0.0%	100.0%	1.0%	5.0%	15.0%
2	0.0%	0.0%	0.0%	1.0%	5.0%	15.0%
3	0.0%	0.0%	0.0%	1.0%	5.0%	15.0%
4	0.0%	0.0%	0.0%	1.0%	5.0%	15.0%
5	0.0%	0.0%	0.0%	1.0%	5.0%	15.0%
6	0.0%	0.0%	0.0%	1.0%	5.0%	15.0%
7	70.0%	0.0%	0.0%	1.0%	5.0%	15.0%
8	80.0%	70.0%	0.0%	1.0%	100.0%	15.0%
9	90.0%	80.0%	70.0%	1.0%	5.0%	15.0%
10	80.0%	70.0%	0.0%	1.0%	5.0%	15.0%
11	70.0%	0.0%	0.0%	1.0%	5.0%	15.0%
12	0.0%	0.0%	0.0%	1.0%	5.0%	15.0%
13	0.0%	0.0%	0.0%	1.0%	5.0%	15.0%
14	0.0%	0.0%	0.0%	1.0%	5.0%	15.0%
15	0.0%	0.0%	0.0%	1.0%	5.0%	15.0%
16	0.0%	0.0%	0.0%	1.0%	5.0%	15.0%
17	0.0%	0.0%	0.0%	1.0%	5.0%	15.0%
18	0.0%	0.0%	0.0%	1.0%	5.0%	15.0%
19	0.0%	0.0%	0.0%	1.0%	5.0%	15.0%
20	0.0%	0.0%	0.0%	1.0%	5.0%	15.0%

Confident that the calculator works as expected with matched panels, we move to measurements where the panel array is partially shaded and the panel parameters vary within the specifications of the manufacturer. The panel shading and mismatch due to manufacturing tolerance percentages used for the calculation are presented in Tables 3 and 4.

The comparison was first performed over a period of one week to compare results between averaged hourly data and more precise per minute data. The main goal here was to determine whether the hourly data would yield sufficient accuracy to be used to simulate the energy over a whole year. The week selected was the 7 day period between 21/4/2009 and 27/4/2009. The results are shown in Table 5 and in Figures 23 and 24.

The results indicate that the use of the lower resolution yields an error that has an absolute value between 0.59% and 0.92%. This is an acceptable error, especially since it is very similar for all the configurations. From now on all results are presented with one hour resolution. It can also be seen from Figures 23 and 24 that the one hour estimate is close to the one minute result. The curves for the first day are almost identical and the curves for the other other days are also similar in both calculations.

The next simulation results are from a simulation with insolation data from

Table 4: Panel array manufacturing mismatch percentages used in the calculation

string / panel	1	2	3	4	5	6
1	1.92%	4.51%	-8.30%	2.86%	0.72%	2.79%
2	-0.01%	-1.14%	-5.46%	0.71%	7.40%	-1.43%
3	-0.40%	-6.02%	-1.62%	-1.08%	2.92%	-1.72%
4	-2.74%	-8.01%	5.70%	1.70%	-3.16%	2.15%
5	-1.09%	-2.60%	3.82%	2.72%	1.99%	6.55%
6	-0.50%	-3.20%	10.69%	-4.16%	0.01%	6.58%
7	-0.05%	-4.08%	2.38%	0.42%	-0.43%	-2.65%
8	6.06%	-2.57%	3.31%	6.63%	1.61%	-4.21%
9	-2.11%	-3.21%	1.86%	-0.05%	0.34%	-6.69%
10	8.43%	7.82%	-0.60%	-0.44%	4.30%	-1.64%
11	0.55%	3.21%	-0.59%	2.03%	-1.79%	6.55%
12	1.29%	-6.18%	-10.67%	-2.96%	3.48%	-3.62%
13	1.91%	-2.71%	-7.01%	-7.57%	1.48%	0.44%
14	-0.38%	-0.75%	-0.78%	2.65%	-1.60%	-1.53%
15	-1.97%	2.31%	3.35%	-1.02%	4.71%	7.01%
16	-3.39%	4.61%	2.52%	1.18%	3.65%	-1.63%
17	-9.26%	-2.03%	-0.73%	-7.61%	2.13%	-3.90%
18	-2.88%	-3.71%	-0.63%	4.22%	-2.14%	-0.99%
19	-4.00%	-2.75%	2.72%	0.05%	5.38%	1.57%
20	-3.17%	0.10%	-9.44%	1.70%	4.49%	6.18%

Table 5: Energy yield of different configurations over one week with one hour and one minute resolutions

configuration / resolution	Central Boost	String Boost	Central inv. + transf.
1h	670kWh	769kWh	682kWh
1min	664kWh	762kWh	678kWh
difference	0.90%	0.92%	0.59%

21/4/2009 and 20/4/2010 with one hour resolution. The panel shading and mismatch situation is the same as in the previous simulation. The results are presented in Table 6 and Figure 25.

The results clearly show that the string boost configuration yields more energy than the other configurations in a scenario where the panel array is partially shaded. Figure 25 indicates that the string boost configuration yields more energy consistently throughout the year.

The inverter with the transformer outputs slightly more energy than the central boost configuration, although it has a slightly smaller efficiency at high power. Its

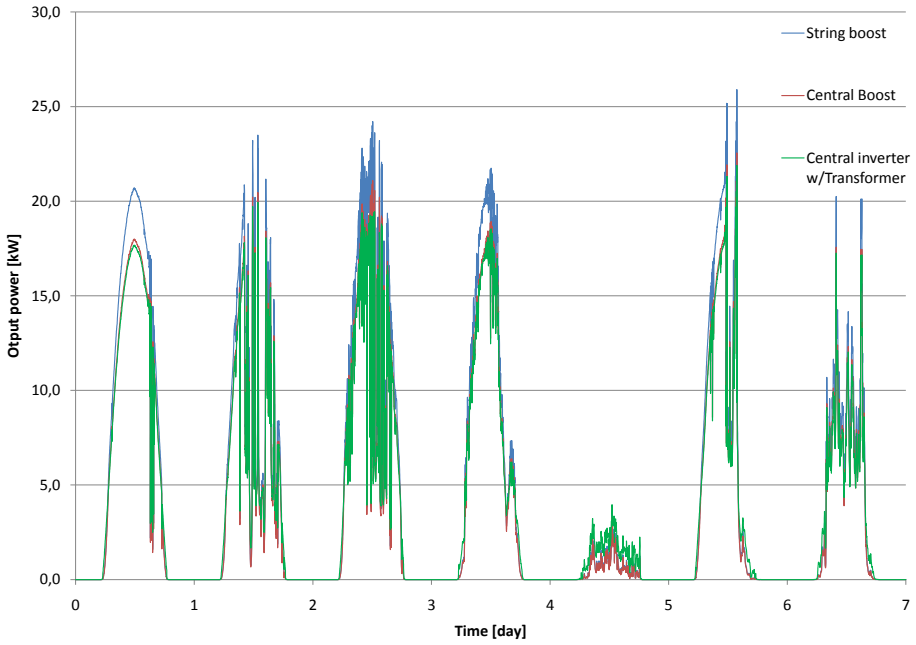

Figure 23: Plant output power as a function of time over a week, 1min resolution

Table 6: Energy yield of different configurations over one year with one hour resolution

	Central Boost	String Boost	Central inv. + transf.
Energy yield	30925kWh	35467kWh	31316kWh
Loss over best	-4542kWh	0kWh	-4151kWh
Loss in %	-12.81%	0.00%	-11.70%

efficiency at very low power, however, is significantly better than any of the other configurations studied. Figures 26 shows the efficiency as a function of time over one year and Figure 27 over one week.

Figure 26 indicates that the efficiency of the transformer configuration is generally lower than that of the other two configurations. However, the close-up of the first week in the calculation shown in Figure 27 shows that the efficiency of the transformer configuration is in fact significantly higher at low power levels. This behaviour is visible in all the calculations.

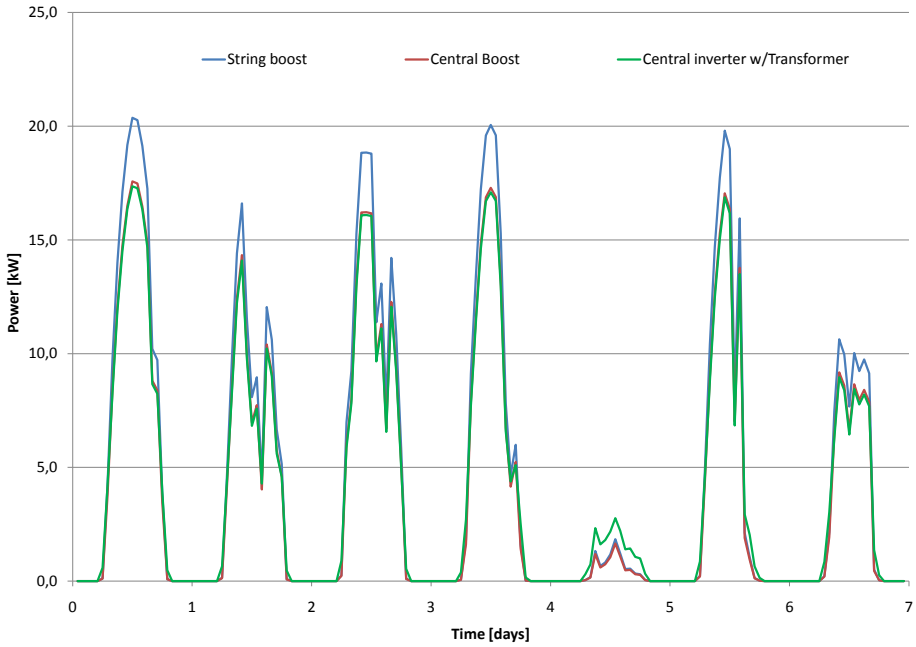

Figure 24: Plant output power as a function of time over a week, one hour resolution

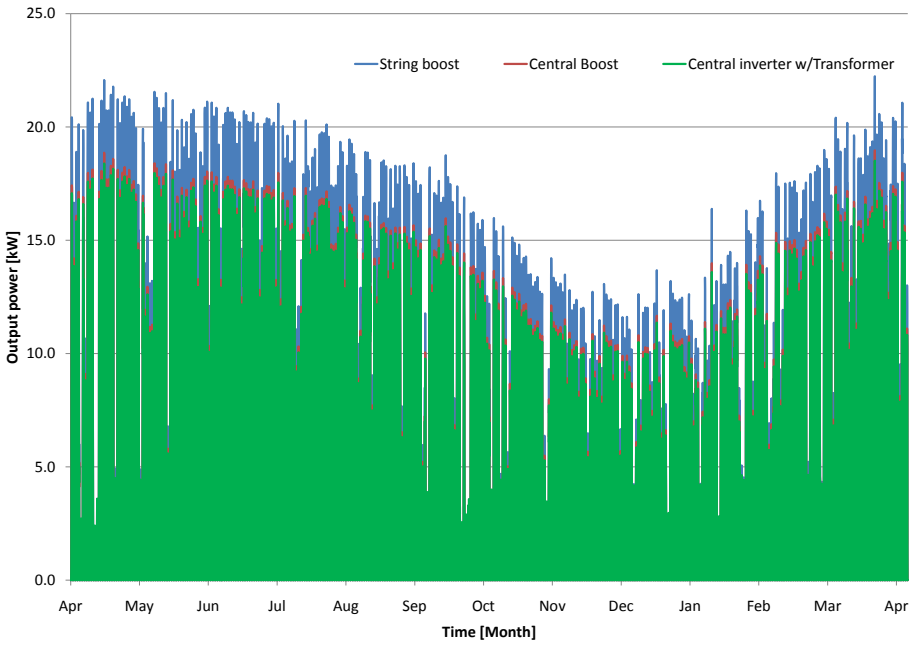

Figure 25: Plant output power as a function of time over a year, one hour resolution

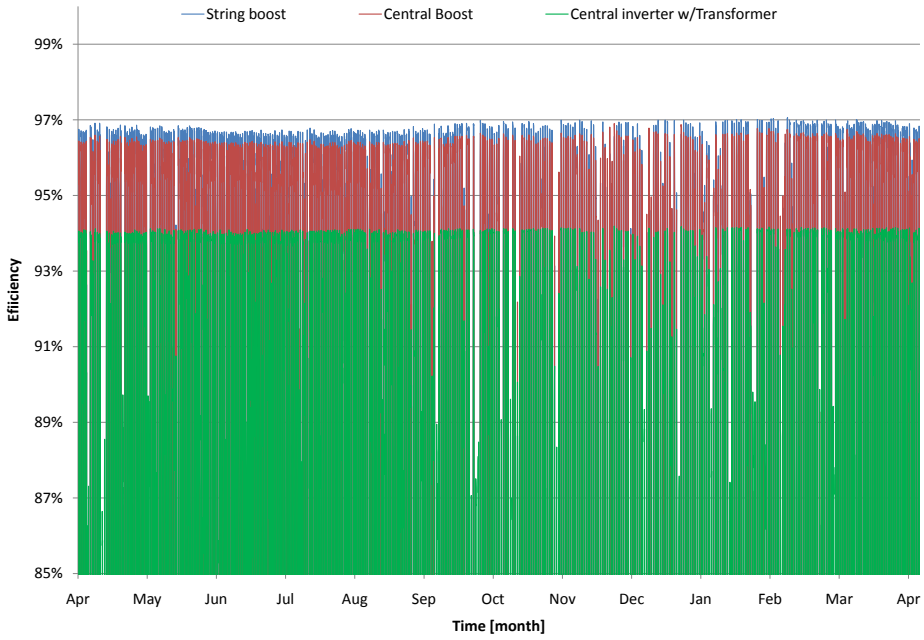

Figure 26: Plant efficiency as a function of time over a year, one hour resolution

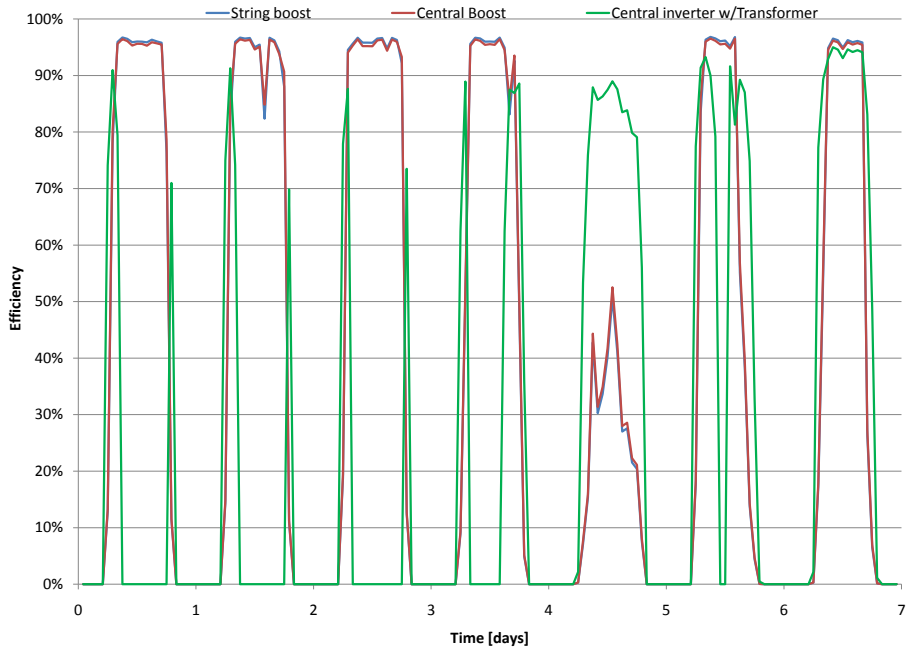

Figure 27: Plant efficiency as a function of time over a week, one hour resolution

4.2 Error analysis

The largest error source in these calculations is the approximation in the voltage-current dependency of the pV-panel. This error is practically impossible to analyse without actual knowledge of the panel. Manufacturers only publish three points in the UI-curve, the short circuit current, the MPP voltage and current, and the open circuit voltage, through which the approximated curve also goes.

In this section we limit ourselves to an analysis of the error in the actual Excel calculator and assume the manufacturer data to be accurate. This is a reasonable assumption since possible errors in this data would be evened out anyway in an installation with 120 panels, such as is under investigation. Comparing the piece-wise linear approximation to the curve that can be derived from the mathematical model is the only way to analyse the error with the available information. The approximated and model-based power curves and their difference curve are plotted in Figure 28.

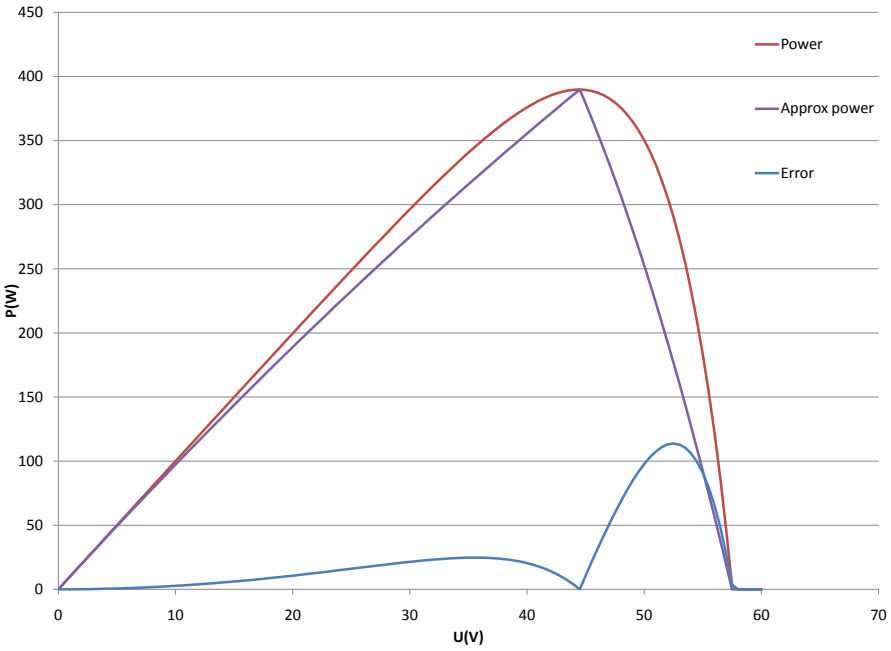

Figure 28: pV-panel power, approximate power, and power error as a function of voltage

The error shown in Figure 28 is that of only one string. If several strings are connected in parallel to form an array, the calculator presented in this thesis will find the global MPP of the whole array. The maximum error presents itself when a string is producing less than half of its maximum power. For this point to be the global MPP, the other strings would have to be very near their MPP. Since high-power strings have a small error, low-power strings have a large error, and the output is the sum of the power integrated over time, it can be said that strings which present a large error have less weight in the output than strings with a small

error. Therefore the error of more than 30% shown in Figure 28 will never be the error of the whole system. The accumulation of the total error will be explained next and detailed calculations will follow.

The calculator used in this thesis accepts up to six individual strings. Five out of six strings would thus have a very small error in power and only one string would have an error of 40%. Assuming the strings would have the same power at MPP, the error in power would be much smaller, less than 10%, since the error of the higher power strings would be very small. If two or more out of six strings would have their maximum error point at the maximum power point of the remaining strings, the MPP of the whole array would be at the MPP of those two strings. This can be verified by noting that the MPP-voltage is 85% of the voltage at the maximum error and the power at this voltage is 86% of the maximum power, and that the power at the maximum error is 45% of the maximum power. These values correspond to Figure 28.

If two weaker strings had their MPP at 85% of the remaining four stronger strings, the total power of the system, if operating at the MPP of the stronger strings, would be

$$P = 4 \cdot P_{MPP} + 2 \cdot P_{e_{max}} \tag{31}$$
$$= 4 \cdot P_{MPP} + 2 \cdot 0.45 \cdot P_{MPP} \tag{32}$$
$$= 4.9 \cdot P_{MPP}. \tag{33}$$

If, on the other hand, the system would be operating at the MPP of the two weaker strings, the power would be approximately

$$P = 6 \cdot 0.86 \cdot P_{MPP} \tag{34}$$
$$= 5.16 \cdot P_{MPP}. \tag{35}$$

Since the latter power is larger, the calculator assumes that operating point, and the error of the other operating point becomes irrelevant.

Let us first derive the error in the case where one string out of six has an MPP-voltage that is 15% smaller than the rest.

$$\Delta P = (5 \cdot P_{MPP} + P_{e_{max}}) - (5 \cdot \hat{P}_{MPP} + \hat{P}_{e_{max}}) \tag{36}$$

The error of the strings operating at the MPP is zero

$$\Delta P = P_{e_{max}} - \hat{P}_{e_{max}} \tag{37}$$
$$\Delta P_{\%} = \frac{P_{e_{max}} - \hat{P}_{e_{max}}}{5 \cdot \hat{P}_{MPP} + \hat{P}_{e_{max}}} \cdot 100\% \tag{38}$$

The values corresponding to Figure 28 are

$$= \frac{113.7W}{2125.8W} \cdot 100\% \tag{39}$$
$$\approx 5.3\% \tag{40}$$

Based on the deduction above, this is the largest error that can be caused by a string operating at the maximum error point.

Let us now investigate a case where three panels have an MPP-voltage 15% lower than the other three. The error of the whole system would be

$$\Delta P = (3 \cdot P_{MPP} + 3 \cdot P_{85\%MPP}) - (3 \cdot \hat{P}_{MPP} + 3 \cdot \hat{P}_{85\%MPP}) \tag{41}$$

There is no error at the MPP so

$$\hat{P}_{MPP} = P_{MPP} \tag{42}$$

$$\Delta P = 3 \cdot \left(P_{85\%MPP} - \hat{P}_{85\%MPP} \right) \tag{43}$$

$$\Delta P_{\%} = \frac{\Delta P}{\hat{P}} = \frac{3 \cdot \left(P_{85\%MPP} - \hat{P}_{85\%MPP} \right)}{6 \cdot \hat{P}_{85\%MPP}} \cdot 100\% \tag{44}$$

$$= \frac{1}{2} \left(\frac{P_{85\%MPP}}{\hat{P}_{85\%MPP}} - 1 \right) \cdot 100\% \tag{45}$$

$$= \frac{1}{2} \left(\frac{360W}{336W} - 1 \right) \cdot 100\% \tag{46}$$

$$\approx 3.6\% \tag{47}$$

This value is smaller than the value in (40), so the 5.1% is considered to be the maximum error caused by the approximation of the UI-curve.

Let us now continue to calculate the total error of the calculation. The output of the simulation is energy, which is calculated as follows.

$$E = I_0 \frac{S}{S_0} \cdot U_0 \frac{T}{T_0} \cdot t \tag{48}$$

$$= P_0 \frac{ST}{S_0 T_0} \cdot t \ , \tag{49}$$

The error in E can now be estimated to be

$$\frac{\Delta E}{E} = \frac{\partial}{\partial P_0} \frac{P_0}{Pt} \frac{ST}{S_0 T_0} \cdot t \cdot \Delta P_0 + \underbrace{\frac{\partial}{\partial S_0} \frac{P_0}{Pt} \frac{ST}{S_0 T_0} \cdot t \cdot \Delta S_0 + \frac{\partial}{\partial T_0} \frac{P_0}{Pt} \frac{ST}{S_0 T_0} \cdot t \cdot \Delta T_0}_{\approx 1\% \text{ (see Table 5)}} \tag{50}$$

$$ST \approx S_0 T_0 \Rightarrow \tag{51}$$

$$\Delta E_{\%} \approx \frac{\Delta P_0}{P} \cdot 100\% + 1\% = 5.3\% + 1\% \tag{52}$$

$$= 6.3\% \tag{53}$$

This is the error if the energy of an array with a single MPPT is calculated. If each string has its own MPPT, the error will only be the 1% quantification error caused by the use of hourly data instead of per minute data, since the string will always be operating at its MPP, where the linearisation does not introduce any error. This is of course assuming that the values claimed by the manufacturer are accurate.

In other words the 6.3% error only applies to the central boost and transformer configurations, whereas the string boost configuration calculation is more accurate with an error of only 1%.

Another source of error is introduced by the efficiency maps used in the simulation. However, the efficiency maps can be provided by the user so it is not sensible to consider their effects in great length here.

5 Summary and discussion

The basic properties of photovoltaic panels were discussed in the beginning of this thesis. The current is almost constant at low voltage, but starts dropping exponentially shortly before the maximum power point of the panel. PV-panel short circuit current is proportional to solar irradiation and open circuit voltage inversely proportional to pV-cell temperature. It was shown that the described properties of pV-panels introduce some challenges to large-scale energy production, where 3-phase AC grids are almost exclusively used, panels are connected in series to form strings and strings are potentially connected in parallel to form arrays.

The advantages and disadvantages of the power converter configurations were subsequently discussed. Single stage inverters have a high efficiency, but have trouble coping with the voltage variations caused by temperature changes. Boost converter fed inverters overcome the issues with voltage variations and add the possibility to track the MPP of individual strings.

It became evident that choosing a suitable configuration is non-trivial and that some sort of simulation, or other calculation, could prove to be a great aid in evaluating the actual energy yield of different configurations. Measurements were made to confirm the claimed efficiencies of power converters. A very similar measurement set-up was later used in the prototyping stage of a new inverter product.

The next section described the development and functionality of a tool made especially to calculate and compare the energy yields of different configurations in known insolation and temperature conditions. The user also has the possibility to introduce shading differences and manufacturing mismatches to the panel installation.

The Excel calculation tool presented in this thesis shows that if there is partial shading in the installation, different inverter configurations will yield different amounts of energy. This is an expected result and agrees with publications and manufacturer claims. Therefore, the calculation tool presented can help determine whether or not the difference between a more expensive and complex configuration merits the added cost.

Based on the results, it became very clear that the ranking order of the configurations depends on the amount of partial shading. If significant partial shading is present one configuration is clearly above the rest. However, if no shading is present at all, the configurations yield very similar results. In moderate climates it might also be possible to leave out the boost converter stage all together. Suitable areas are scarce, but they exist where large bodies of water moderate both winters and summers. As speculated in the beginning of this thesis, there is no globally optimal configuration.

A browse of the catalogue of the German solar inverter manufacturer SMA shows that the company aims to solve the issue by offering dozens of models for different kinds of installations. Another, perhaps logistically simpler, option might be to offer a scalable inverter unit and multiple front-ends to choose from. These front-ends might take care of voltage boosting or galvanic isolation, or both. The number of boost converters could also be varied depending on the likelihood of partial shading.

The aim of this thesis was not to determine the best solution for a given set of parameters either, but to give a universal tool to do so for any set of parameters. This aim was reached. The tool is reasonably fast, the comparison of different configurations over a year can be done in less than a minute. All relevant data, such as insolation, temperature panel shading, and system efficiency data can be input by the user, and most of all, the calculator gives a good approximation of the energy yield of the configurations in question. The tool was used to make decisions about the guidelines of a new product line.

During the development and finalisation of this thesis, several improvements were made to the original calculation tool. Some features, however, were purposefully left out. Among these is the ability to use a more exact model of the pV-cell rather than the piecewise linear approximation. The use of such a model might well lead to a necessity to optimize the algorithms to run faster. It might even render the use of Excel impossible, because of the limitations of the VBA programming language and amount of data needed. Further development outside Excel would clearly be outside the scope of this thesis, but leaves interesting questions for further research.

It would be very interesting to find a solar panel installation site, where measured temperature and insolation data along with the energy output would be available. This data could be used to verify the presented calculator with real data. Ideally, information of the shading of each individual panel would also be available. Regrettably solar installations in Finland are rare. Sites where all the previous measurements would be made are even more rare.

Some interesting points also came out in investigating the literature for this thesis. One is the fact that standard IEC 60364-7-712 defines the maximum voltage of an installation to be the open circuit voltage at STC-conditions. This means that the panel is at 25°C. In Nordic countries and mountainous regions the ambient temperature can fall well below -20°C. At this temperature the open circuit voltage might be about 15% higher. While the insolation and thus the current in these conditions are not likely to produce large amounts of energy, the voltage could certainly be high enough to cause a breakdown in the capacitors used in the converter, especially if the capacitors were dimensioned with little headroom. Of course the installer of the panels could take this into account, but it should be the purpose of the standard to ensure safe installations.

Another interesting fact is that accurate measurement data of the voltage-current behaviour of pV-modules is almost impossible to find. Surely this information exists since it is the only accurate way to determine the MPP of a module, and the voltage and current at that point are regularly stated in the specifications of panels. This measurement data would be very important in validating models and building identification based models.

References

[1] B. Richards and M. Watt, "Permanently dispelling a myth of photovoltaics via the adoption of a new net energy indicator," *Renewable and Sustainable Energy Reviews*, vol. 11, no. 1, 2007, pp. 162–172.

[2] BP, *230W Photovoltaic module BP 3230T*. [Online]. Available: http://www.bp.com/liveassets/bp_internet/solar/bp_solar_usa/STAGING/local_assets/downloads_pdfs/pq/BP3230T_1-10.pdf

[3] T. Markvart(edit.), *Solar Electricity (Energy Engineering Learning Package)*. Chichester, England: John Wiley & Sons, 1994.

[4] F. A. Farret and M. G. Simões, *Integration of Alternative Sources of Energy*. Hoboken, NJ: Wiley-IEEE Press, 2006.

[5] J. Lesser and N. Puga, "PV vs. solar thermal," *Public Utilities Fortnightly*, Jul. 2008. [Online]. Available: http://www.fortnightly.com

[6] G. Walker, "Evaluating MPPT converter topologies using a MATLAB PV model," *Journal of Electrical & Electronics Engineering, Australia*, vol. 21, no. 1, 2001, pp. 49–55.

[7] H. Patel and V. Agarwal, "MATLAB-based modeling to study the effects of partial shading on PV array characteristics," *IEEE Transactions on Energy Conversion*, vol. 23, no. 1, 2008, pp. 302–10.

[8] W. Shokley, "The theory of p-n junctions in semiconductors and p-n junction transistors," *Bell System Technical Journal*, vol. 28, no. 3, Jul. 1949, pp. 435–489.

[9] T. Nordmann and L. Clavadetscher, "Understanding temperature effects on pv system performance," *Proceedings of 3rd World Conference on Photovoltaic Energy Conversion, 2003.*, vol. 3, May 2003, pp. 2243–2246.

[10] *Photovoltaic devices - Part 3: Measurement principles for terrestrial photovoltaic (PV) solar devices with reference spectral irradiance data*, IEC60 904-3-Ed.2.0, 2008.

[11] T. Esram and P. Chapman, "Comparison of photovoltaic array maximum power point tracking techniques," *IEEE Transactions on Energy Conversion*, vol. 22, no. 2, Jun. 2007, pp. 439–449.

[12] V. Salas, M. Alonso-Abellá, F. Chenlo, and E. Olías, "Analysis of the maximum power point tracking in the photovoltaic grid inverters of 5 kw," *Renewable Energy*, vol. 34, no. 11, 2009, pp. 2366–2372.

[13] aleo solar AG, "aleo s_18 solar module datasheet," 2010. [Online]. Available: http://www.aleo-solar.de/images/documents/datenblaetter/datenblaetter_aleo/S18%20220_3%20EN%20DE.pdf

[14] A. Woyte, J. Nijs, and R. Belmans, "Partial shadowing of photovoltaic arrays with different system configurations: literature review and field test results," *Solar Energy*, vol. 74, no. 3, 2003, pp. 217–233.

[15] T. L. Nguyen and K.-S. Low, "A global maximum power point tracking scheme employing direct search algorithm for photovoltaic systems," *IEEE Transactions on Industrial Electronics*, vol. 57, no. 10, Oct. 2010, pp. 3456–3467.

[16] S. Kjaer, J. Pedersen, and F. Blaabjerg, "A review of single-phase grid-connected inverters for photovoltaic modules," *IEEE Transactions on Industry Applications*, vol. 41, no. 5, 2005, pp. 1292–1306.

[17] Y. Huang, F. Peng, J. Wang, and D. Yoo, "Survey of the power conditioning system for PV power generation," in *Power Electronics Specialists Conference, 2006. PESC'06. 37th IEEE*. IEEE, 2006, pp. 1–6.

[18] B. K. t. Bose, *Power Electronics and Variable Frequency Drives: Technology and Applications*. Piscataway, NJ, USA: Wiley-IEEE Press, 1996.

[19] I. Boldea and S. A. Nasar, *Electric Drives*. Boca Raton, FL, USA: CRC Press, 1999.

[20] *Electrical installations of buildings - Part 7-712: Requirements for special installations or locations - Solar photovoltaic (PV) power supply systems*, IEC60 364-7-712, 2002.

[21] M. Liukkonen, A. Hentunen, and J. Suomela, "Analysis of the ultracapacitor module in power buffering," in *Proceedings of 4th European Symposium on Super Capacitors & Applications*, Bordeaux, France, Oct. 2010, p. (in press).

[22] SMA, *Sunny Mimi Central Installation guide*. [Online]. Available: http://download.sma.de/smaprosa/dateien/5710/SMC9-11TLRP-IEN100640.pdf

[23] *Article 690: Solar PV Systems, National Electrical Code*, ANSI/NFPA-70 National Fire Protection Association, Inc. Quincy, MA, 2008.

[24] K. Kobayashi, I. Takano, and Y. Sawada, "A study on a two stage maximum power point tracking control of a photovoltaic system under partially shaded insolation conditions," vol. 4, Jul. 2003, p. 2617.

[25] K. T. Gribbon and D. G. Bailey, "A novel approach to real-time bilinear interpolation," *Second IEEE International Workshop on Electronic Design, Test and Applications, DELTA 2004*, 2004, pp. 126–131.

[26] S. R. R. Laboratory. (2010, Apr.) Baseline measurement system, daily data & plots. [Online]. Available: http://www.nrel.gov/midc/srrl_bms/

Appendix A: Validation Data

Table A1: Excel tool validation data

Excel						Simulink		
Irradiation	Tamb	Tpv	Vmpp	Impp	Pmpp	Vmpp	Impp	Pmpp
-5.30	10.37	10.22	0.00	0.00	0.00	0.00	0.00	0.00
-4.11	9.64	9.52	0.00	0.00	0.00	0.00	0.00	0.00
-4.27	8.88	8.76	0.00	0.00	0.00	0.00	0.00	0.00
-5.06	8.25	8.11	0.00	0.00	0.00	0.00	0.00	0.00
-5.30	10.37	10.22	0.00	0.00	0.00	0.00	0.00	0.00
-4.11	9.64	9.52	0.00	0.00	0.00	0.00	0.00	0.00
-4.27	8.88	8.76	0.00	0.00	0.00	0.00	0.00	0.00
-5.06	8.25	8.11	0.00	0.00	0.00	0.00	0.00	0.00
-2.93	8.65	8.57	0.00	0.00	0.00	0.00	0.00	0.00
29.97	8.74	9.57	193.66	0.63	121.29	453.06	0.56	255.19
206.07	11.83	17.52	628.96	4.31	2708.59	564.65	4.20	2372.93
423.17	14.88	26.58	614.43	8.84	5433.62	585.61	8.75	5125.05
627.61	16.52	33.87	603.56	13.12	7916.17	590.25	13.06	7707.31
802.03	17.59	39.77	594.63	16.76	9966.50	589.53	16.74	9869.98
932.30	19.08	44.86	585.33	19.48	11404.18	585.29	19.50	11412.31
1000.50	19.31	46.98	582.09	20.91	12170.55	584.09	20.94	12233.30
993.55	20.07	47.55	579.86	20.76	12039.71	582.17	20.80	12106.65
918.81	20.30	45.70	581.87	19.20	11172.62	582.09	19.21	11183.89
801.65	21.21	43.38	583.02	16.75	9767.26	579.61	16.74	9700.09
438.97	20.88	33.01	595.41	9.17	5461.98	569.69	9.08	5175.24
402.66	21.58	32.71	594.26	8.41	5000.54	565.05	8.32	4701.85
182.56	20.30	25.35	603.83	3.82	2303.68	534.73	3.71	1985.25
21.01	17.76	18.34	130.24	0.44	57.18	407.07	0.38	156.10
-4.80	14.87	14.74	0.00	0.00	0.00	0.00	0.00	0.00
-4.23	14.03	13.91	0.00	0.00	0.00	0.00	0.00	0.00
-3.80	13.25	13.14	0.00	0.00	0.00	0.00	0.00	0.00
-3.56	12.50	12.40	0.00	0.00	0.00	0.00	0.00	0.00
-5.14	14.33	14.19	0.00	0.00	0.00	0.00	0.00	0.00
-4.12	13.58	13.47	0.00	0.00	0.00	0.00	0.00	0.00
-4.55	12.67	12.54	0.00	0.00	0.00	0.00	0.00	0.00
-4.06	11.70	11.59	0.00	0.00	0.00	0.00	0.00	0.00
-3.78	11.65	11.55	0.00	0.00	0.00	0.00	0.00	0.00
4.50	11.34	11.47	28.81	0.09	2.71	283.24	0.06	18.37
111.10	12.61	15.68	628.58	2.32	1459.46	528.57	2.23	1177.55
306.05	15.96	24.43	614.05	6.40	3927.40	570.65	6.29	3591.54
506.96	19.76	33.78	596.93	10.59	6324.05	576.73	10.52	6064.42
702.92	21.35	40.79	585.88	14.69	8606.43	578.33	14.65	8471.02
873.22	22.14	46.28	577.55	18.25	10539.33	577.37	18.25	10535.42
988.66	22.92	50.25	570.76	20.66	11792.42	574.81	20.69	11893.51
1039.77	24.63	53.38	563.18	21.73	12237.44	569.93	21.78	12410.72
1035.90	25.96	54.60	558.97	21.65	12100.63	566.65	21.69	12292.27
976.45	26.95	53.95	558.07	20.41	11387.84	564.65	20.43	11537.63
859.17	28.06	51.81	558.94	17.95	10035.66	562.09	17.95	10090.62
686.77	28.41	47.40	564.00	14.35	8094.56	559.53	14.31	8005.44
494.30	28.05	41.71	571.47	10.33	5903.18	553.93	10.25	5677.18
258.28	26.24	33.38	583.89	5.40	3151.56	535.53	5.29	2834.68
80.13	24.70	26.92	476.10	1.67	797.24	478.26	1.59	759.67
-0.43	23.42	23.41	0.00	0.00	0.00	0.00	0.00	0.00
-4.07	22.20	22.09	0.00	0.00	0.00	0.00	0.00	0.00
-4.19	21.21	21.10	0.00	0.00	0.00	0.00	0.00	0.00
-4.33	19.72	19.60	0.00	0.00	0.00	0.00	0.00	0.00
Energy:					201.88kWh			199.35kWh

Appendix B: Efficiency tables

Table B1: DC-AC inverter efficiency data (estimated)

$U^{DC}_{p.u.}$ \ $I_{p.u.}$	0	0.033	0.5	1.3
1	5%	93%	98%	98%
1.1	5%	92%	97%	96%
1.2	5%	91%	96%	95%
1.3	5%	90%	95%	94%
1.4	5%	89%	94%	93%
1.5	5%	88%	93%	92%
1.6	5%	87%	92%	91%
1.7	5%	86%	91%	90%
1.8	5%	85%	90%	89%
1.9	5%	84%	89%	88%
2.0	5%	83%	88%	87%

Table B2: Step-up transformer efficiency measurement data

Power p.u.	0.0	0.0	0.1	0.1	0.2	0.2	0.3	0.4	0.6	0.8	0.9	1.0
Efficiency %	0.00	77.42	91.57	94.31	95.95	96.25	97.16	97.90	97.91	98.09	97.93	97.86

Table B3: DC-DC converter efficiency measurement data, measured up to 58%

$\frac{U_{in}}{U_{out}}$ \ $I_{p.u.}$	0.00	0.25	0.41	0.58	0.74	0.90	1.07	1.23	1.43	1.64
0	0.00%	0.00%	0.00%	0.00%	0.00%	0.00%	0.00%	0.00%	0.00%	0.00%
0.01	0.00%	55.00%	60.00%	60.00%	60.00%	0.00%	0.00%	0.00%	0.00%	0.00%
0.02	0.00%	70.00%	75.00%	75.00%	73.00%	0.00%	0.00%	0.00%	0.00%	0.00%
0.03	0.00%	77.00%	81.00%	82.00%	81.00%	98.54%	0.00%	90.48%	0.00%	0.00%
0.04	0.00%	80.00%	84.50%	85.00%	85.00%	93.33%	92.14%	89.70%	87.27%	87.57%
0.05	0.00%	83.00%	86.50%	87.00%	87.00%	92.02%	90.26%	88.79%	88.50%	87.70%
0.06	0.00%	84.50%	88.00%	88.50%	88.50%	92.08%	90.77%	89.82%	89.56%	87.68%
0.07	0.00%	86.00%	89.00%	89.50%	90.00%	94.07%	93.19%	89.70%	89.76%	88.60%
0.08	0.00%	87.00%	90.00%	90.50%	90.50%	92.33%	92.50%	89.51%	90.30%	89.39%
0.09	0.00%	88.00%	90.00%	91.00%	91.00%	92.60%	91.68%	91.35%	90.73%	90.10%
0.1	0.00%	88.50%	91.00%	91.50%	92.00%	93.06%	92.25%	91.99%	91.20%	90.71%
0.11	0.00%	89.00%	91.00%	92.00%	92.00%	93.36%	92.70%	92.30%	91.67%	91.20%
0.12	0.00%	89.50%	92.00%	92.00%	93.00%	93.47%	93.14%	92.54%	92.48%	91.67%
0.13	0.00%	90.00%	92.00%	93.00%	93.00%	93.75%	93.48%	93.08%	92.70%	92.36%
0.14	0.00%	90.00%	92.00%	93.00%	93.00%	93.99%	93.79%	93.50%	92.94%	92.70%
0.15	0.00%	90.50%	93.00%	93.00%	93.50%	94.24%	94.00%	93.70%	93.46%	93.00%
0.16	0.00%	91.00%	93.00%	93.00%	94.00%	94.48%	94.15%	93.87%	93.80%	93.40%
0.17	0.00%	91.00%	93.00%	94.00%	94.00%	94.65%	94.39%	94.20%	93.96%	93.67%
0.18	0.00%	91.00%	93.00%	94.00%	94.00%	94.71%	94.54%	94.61%	94.43%	94.00%
0.19	0.00%	91.50%	93.50%	94.00%	94.00%	94.91%	94.97%	94.80%	94.80%	94.22%
0.2	0.00%	92.00%	94.00%	94.00%	95.00%	95.16%	95.33%	94.93%	95.22%	94.35%
0.21	0.00%	92.00%	94.00%	94.00%	95.00%	95.54%	95.13%	95.01%	94.81%	94.50%
0.22	0.00%	92.00%	94.00%	95.00%	95.00%	95.26%	95.31%	95.24%	95.00%	94.64%
0.23	0.00%	92.00%	94.00%	95.00%	95.00%	95.43%	95.48%	95.33%	95.08%	94.80%
0.24	0.00%	93.00%	94.00%	95.00%	95.00%	95.59%	95.59%	95.40%	95.25%	94.97%
0.25	0.00%	93.00%	94.00%	95.00%	95.00%	95.70%	95.72%	95.51%	95.40%	95.22%
0.26	0.00%	93.00%	94.44%	95.61%	95.80%	95.82%	95.82%	95.69%	95.45%	95.30%
0.27	0.00%	93.09%	94.52%	95.69%	95.88%	95.96%	95.90%	95.79%	95.67%	95.43%
0.28	0.00%	93.29%	94.66%	95.79%	95.96%	96.09%	95.98%	95.96%	95.78%	95.60%
0.29	0.00%	93.38%	94.83%	95.88%	96.07%	96.15%	96.06%	96.09%	95.90%	95.65%
0.3	0.00%	93.46%	94.91%	95.98%	96.14%	96.28%	96.15%	96.20%	95.95%	95.84%
0.31	0.00%	93.57%	95.03%	96.05%	96.25%	96.30%	96.23%	96.17%	96.15%	95.90%
0.32	0.00%	93.60%	95.14%	96.10%	96.29%	96.42%	96.41%	96.31%	96.30%	96.02%
0.33	0.00%	93.68%	95.21%	96.19%	96.39%	96.54%	96.44%	96.43%	96.29%	96.16%
0.34	0.00%	93.74%	95.35%	96.21%	96.45%	96.57%	96.52%	96.51%	96.42%	96.30%
0.35	0.00%	93.85%	95.34%	96.32%	96.47%	96.64%	96.62%	96.59%	96.55%	96.31%
0.36	0.00%	93.95%	95.51%	96.35%	96.57%	96.68%	96.71%	96.73%	96.60%	96.46%
0.37	0.00%	94.05%	95.65%	96.40%	96.64%	96.74%	96.77%	96.80%	96.64%	96.60%
0.38	0.00%	94.15%	95.60%	96.47%	96.71%	96.79%	96.82%	96.83%	96.77%	96.55%
0.39	0.00%	94.15%	95.70%	96.52%	96.79%	96.95%	96.87%	96.90%	96.82%	96.67%
0.4	0.00%	94.30%	95.82%	96.61%	96.82%	96.99%	96.95%	96.92%	96.90%	96.70%
0.41	0.00%	94.34%	95.92%	96.62%	96.87%	97.04%	96.99%	97.00%	96.89%	96.75%
0.42	0.00%	94.38%	95.98%	96.69%	96.96%	97.09%	97.32%	97.74%	97.00%	97.25%
0.43	0.00%	94.45%	96.02%	96.75%	97.00%	97.11%	97.30%	97.13%	97.28%	97.10%
0.44	0.00%	94.52%	96.15%	96.85%	97.31%	97.18%	97.23%	97.20%	97.30%	96.98%
0.45	0.00%	94.58%	96.18%	96.83%	97.11%	97.24%	97.27%	97.25%	97.16%	97.06%
0.46	0.00%	94.64%	96.25%	96.90%	97.14%	97.28%	97.31%	97.40%	97.24%	97.10%
0.47	0.00%	94.71%	96.30%	96.93%	97.18%	97.33%	97.40%	97.38%	97.29%	97.12%
0.48	0.00%	94.82%	96.37%	96.98%	97.22%	97.38%	97.43%	97.42%	97.31%	97.26%
0.49	0.00%	94.89%	96.48%	97.03%	97.27%	97.48%	97.47%	97.45%	97.40%	97.30%
0.5	0.00%	94.92%	96.49%	97.06%	97.34%	97.51%	97.58%	97.48%	97.45%	97.29%
0.51	0.00%	95.01%	96.58%	97.12%	97.36%	97.55%	97.60%	97.51%	97.50%	97.36%
0.52	0.00%	95.10%	96.67%	97.14%	97.41%	97.57%	97.65%	97.62%	97.51%	97.40%
0.53	0.00%	95.21%	96.74%	97.20%	97.46%	97.61%	97.63%	97.65%	97.40%	97.40%
0.54	0.00%	95.27%	96.78%	97.22%	97.46%	97.60%	97.66%	97.66%	97.27%	97.40%
0.55	0.00%	95.34%	96.81%	97.23%	97.50%	97.68%	97.65%	97.70%	97.30%	97.40%
0.56	0.00%	95.48%	96.88%	97.27%	97.51%	97.70%	97.21%	97.70%	97.30%	97.40%
0.57	0.00%	95.53%	96.91%	97.31%	97.49%	96.70%	97.20%	97.70%	97.30%	97.40%
0.58	0.00%	95.62%	96.96%	97.30%	97.50%	95.60%	97.20%	97.70%	97.30%	97.40%
1	0.00%	99.50%	99.50%	99.50%	99.50%	99.50%	99.50%	99.50%	99.50%	99.50%